

NASA CR-143808

X-7ra
COD

EUV AND X-RAY SPECTROHELIOGRAPH STUDY

E.D. KNOX
R.A. PASTOR
A.L. SALAMON
A.A. STERK

General Electric Company
Space Systems Department
Valley Forge Space Center
P.O. Box 8555
Philadelphia, Pennsylvania 19101

February 1975
Final Report



Prepared for:

GODDARD SPACE FLIGHT CENTER
Greenbelt, Maryland 20771

1. Report No.	2. Government Accession No.	3. Recipient's Catalog No.	
4. Title and Subtitle EUV AND X-RAY SPECTROHELIOGRAPH STUDY		5. Report Date	
		6. Performing Organization Code	
7. Author(s) E. Knox, R. Pastor, A. Salamon, A. Sterk		8. Performing Organization Report No.	
9. Performing Organization Name and Address General Electric Company-Space Systems Dept. Valley Forge Space Center P. O. Box 8555 Philadelphia, Pennsylvania 19101		10. Work Unit No.	
		11. Contract or Grant No. NAS5-20545	
12. Sponsoring Agency Name and Address Milton W. Kalet, Code 680 Technical Officer Goddard Space Flight Center Greenbelt, Maryland 20771		13. Type of Report and Period Covered Final Report June 1974-January 1975	
		14. Sponsoring Agency Code	
15. Supplementary Notes			
16. Abstract This report documents the results of a seven-month study program which was directed toward the definition of an EUV and X-Ray Spectroheliograph which has significant performance and operational improvements over the OSO-7 instrument. The program investigated methods of implementing selected changes defined by the contract statement of work and incorporated the results of the study into a set of drawings which defines the new instrument. The study program also investigated the EUV detector performance degradation observed during the OSO-7 mission and identified the most probable cause of the degradation.			
17. Key Words (Selected by Author(s)) Extreme Ultraviolet Spectroheliograph Fabry-Perot Etalon; Hydrogen-Alpha Spectroheliograph; X-Ray Spectro- heliograph; Variable Apertures		18. Distribution Statement	
19. Security Classif. (of this report) Unclassified	20. Security Classif. (of this page) Unclassified	21. No. of Pages 106	22. Price*

*For sale by the Clearinghouse for Federal Scientific and Technical Information, Springfield, Virginia 22151.

PREFACE

General Electric Company conducted a study program to investigate methods to be used to incorporate selected changes into the OSO-7 EUV and X-Ray Spectroheliograph design and to define a new instrument based on the methods selected. The incorporation of the selected changes would significantly improve the performance and operational capability of the instrument and provide a baseline design for future missions.

The study program was conducted under NASA/GSFC Contract NAS5-20545 and covered a seven-month period starting in June 1974. The study program was broken into three general categories; namely, Opto-Mechanical Studies; Command, Control and Data Processing Studies; and EUV Detector Degradation Analysis.

The opto-mechanical studies addressed the changes required to incorporate a new EUV telescope and a new X-Ray collimator into the instrument and to increase the spectral range of the instrument to include the wavelength interval between 12 and 64 nanometers. The study also considered the use of the Fabry-Perot Etalon as a means of isolating the Hydrogen-Alpha line for observation and led to the selection of this technique over the OSO-7 type spectrometer.

The command, control and data processing studies addressed the changes to the instrument electronics and position sensors which would result in an expanded operational and data acquisition capability. The capability to process and read-out all science data channels simultaneously was added along with the addition of data compression to the Hydrogen-Alpha data channel. The capability to select a specific position of the EUV carriage, EUV mask, and X-Ray filter wheel and a specific size of the entrance aperture without knowledge of the prior position/size was provided. Also, a feature which permits the EUV car-

PRECEDING PAGE BLANK NOT FILMED

riage to automatically scan about a selected position was incorporated. The capability to enter commands during orbit night was also provided.

The EUV detector degradation analysis addressed the degradation of the EUV detectors during the OSO-7 mission. Detector test data and on-orbit data was reviewed to determine the most probably cause for the observed degradation.

The result of the study program is documented in this final report. In addition, a set of drawings was generated to define the new instrument configuration. The optical elements, sensors, mechanisms, and sensor electronics (including high voltage power supplies) were assembled in a common instrument housing. The design of the assembly is basically complete except for those areas which require interface definition or structural and thermal analyses. The electronics assembly, which will contain the command and control logic, data processing, motor drivers, and low voltage power supplies, will be located remotely from the instrument. The design of this assembly was not attempted due to the need for extensive mechanical and electrical interface definition. Circuit diagrams were prepared to reflect the electronic changes.

TABLE OF CONTENTS

<u>Section</u>		<u>Page</u>
1	INTRODUCTION	1
	1.1 Purpose	1
	1.2 Scope of Work	1
2	OPTO-MECHANICAL STUDIES	3
	2.1 EUV System Study	3
	2.2 Hydrogen - Alpha System Study	9
	2.3 Instrument Housing	17
	2.3.1 Requirements	17
	2.3.2 Housing Design	17
	2.4 Instrument Assembly	18
	2.4.1 Requirements	18
	2.4.2 General Arrangement Drawing	19
	2.4.3 Subassembly and Component Drawings	19
	2.4.4 Drawing Tree	21
	2.5 New Parts and Materials	21
	2.6 Parts Common to OSO-7	22
	2.6.1 Requirements	22
	2.6.2 Identification of Parts	22
	2.6.3 Shelf-Life Limited Components	22
3	COMMAND, CONTROL AND DATA PROCESSING STUDIES	27
	3.1 General Requirements	27
	3.2 Control of EUV Entrance Aperture Mechanism	27
	3.2.1 Modes of Operation	27
	3.2.2 Circuit Description - EUV Entrance Aperture Mechanism	28
	3.3 Control of EUV Carriage	35
	3.3.1 Modes of Operation	35
	3.3.2 Circuit Description - EUV Carriage	36
	3.4 Control of EUV Exit Aperture Mask	45
	3.4.1 Modes of Operation	46
	3.4.2 Circuit Description - EUV Exit Aperture Mask Control	46
	3.5 Control of X-Ray Filter Wheels	49
	3.5.1 Modes of Operation	50
	3.5.2 Circuit Description - X-Ray Filter Wheel Control	50

TABLE OF CONTENTS (Cont'd)

<u>Section</u>	<u>Page</u>
3.6 Data Processing	55
3.7 Timing and Telemetry Circuitry	61
3.8 Electronics Parts	67
3.9 Command List	69
3.10 Telemetry List	69
3.11 Logic Packaging and Power Estimate.	69
3.12 Instrument Power Supply	76
3.13 Position Command Interface Requirements	79
3.14 Special Spacecraft - Spectroheliograph Interface Requirement.	81
3.15 Non-Volatile Memory	81
 4 EUV DETECTOR DEGRADATION STUDY	 83
4.1 Study Summary	83
4.2 Conclusions and Recommendations	87
 5 CALIBRATION AND TEST PROCEDURES	 89
5.1 Requirements	89
5.2 Procedure Review Summary.	89
 6 NEW TECHNOLOGIES	 91
 APPENDIX	
A CONTRACT/REPORT CROSS REFERENCE SUMMARY	93
B EUV ENTRANCE SLIT ANALYSIS.	95
C SPECTROHELIOGRAPH STUDY - PRELIMINARY COMMAND LIST	97
D SPECTROHELIOGRAPH STUDY - PRELIMINARY TELEMETRY LIST	101

LIST OF ILLUSTRATIONS

<u>Figure</u>		<u>Page</u>
2.1-1	EUV Detector Illumination	8
2.2-1	EUV Carriage and H-Alpha Interference	10
2.6-1	Drawing Tree	23
3.2-1	EUV Entrance Aperture Mechanism Logic	29
3.3-1	Carriage Position Logic	37
3.4-1	EUV Mask Position Logic	48
3.5-1	X-Ray Filter Wheel Logic	51
3.6-1	Data Accumulation and Compression Logic	57
3.7-1	Timing Generation and Position TLM Logic	65
4.1-1	Life History for 3 MEMs or OSO-7	84
4.1-2	Life vs. Threshold Setting	85
4.1-3	Life vs. Energy	86

LIST OF TABLES

<u>Table</u>		<u>Page</u>
2.1-1	EUV Exit Slit Sizes.	3
2.1-2	EUV Entrance Slit Sizes	4
2.1-3	Image Height at Rowland Circle	7
2.4-1	Subassemblies Requiring Additional Design Activity.	20
2.4-2	Components Requiring Additional Design Activity.	21
2.5-1	New Parts and Materials	22
2.6-1	Shelf Life Limited Components.	25
3.8-1	New Electronics Parts	68
3.12-1	Power Summary	77
3.15-1	Memory Systems Suppliers	82
4.1-1	EUV Detector Plateau/Threshold Slopes	87
5.2-1	Test Procedure Summary	89

SECTION 1
INTRODUCTION

1.1 PURPOSE

The purpose of this report is to document the results of a study program which was conducted to investigate methods to be used to incorporate selected changes into the OSO-7 EUV and X-Ray Spectroheliograph design and to define a new instrument configuration based on the methods selected. The incorporation of the selected changes would significantly improve the performance and operational capability of the instrument and provide a baseline design for future EUV and X-Ray Spectroheliographs.

1.2 SCOPE OF WORK

The study program was conducted in accordance with NASA/GSFC Contract NAS5-20545. The study items were defined in "Specification for Study" dated January 18, 1974, which was included as an attachment to the contract. A cross reference between the specification study item numbers and the responsive report paragraph numbers is given in Appendix A.

The products of the study program are defined in the following contract end item list. The drawing number for the top assembly of item 1 along with the drawing numbers for items 4 and 5 are given for reference.

1. Set of drawings defining the modified instrument indicating material and process specifications, calibration & test procedures and calculations generated during the study program.
2. Monthly Reports
3. Final Report
4. Preliminary General Arrangement Drawing (47J220792)
5. Final General Arrangement Drawing (47J231440)

SECTION 2
OPTO-MECHANICAL STUDIES

This general class of studies relates to the optical and mechanical design changes required to incorporate selected performance and operations improvement items into an OSO-7 Spectroheliograph type instrument. Design changes to be investigated include the incorporation of a new EUV telescope and X-Ray collimator which will improve the spatial resolution of the instrument, the extension of the EUV spectral range to be observed, and the impact of these changes on associated subsystems, structures and mechanisms.

The results of these studies will be incorporated into a set of drawings defining the new spectroheliograph.

2.1 EUV SYSTEM STUDY

The OSO-7 spectrometer was taken as the basic design configuration. The following changes were specified or evolved during the study:

1. The vertical scan, achieved with the spiral entrance slit was eliminated.
2. The six wavelengths which are detected in the launch lock position and the corresponding exit slit widths were defined as tabulated in Table 2.1-1.

Table 2.1-1
EUV Exit Slit Sizes

Slit No.	Wavelength	Effective Beam Width	Actual Width
1	18.040 nm	.0750 nm	.361 mm
2	21.133	.0469	.213
3	25.510	.0750	.318
4	28.415	.0469	.191
5	30.378	.0750	.297
6	33.541	.0469	.178

3. Entrance slit widths were specified as shown in Table 2.1-2.

Table 2.1-2.
EUV Entrance Slit Sizes

Aperture	Vertical	Horizontal**
1	5 Arc Sec	5 Arc Sec
2	10	5
3	20	5
4	20	8
5	10	8
6	5	8
7*	5	8
8*	10	8
9*	20	8
10*	20	5
11*	10	5
12*	5	5
13	40	5
14	60	5
15	60	8
16	40	8

* Filtered Apertures

** Horizontal direction is parallel to the raster lines and the spectral dispersion (i.e., perpendicular to the grating rulings).

- The EUV telescope focal length was assumed to be 212 cm, instead of the 85.5 cm on OSO-7.
- The desired spectral range was extended to cover the 12.0 to 64.0 nanometer wavelength interval.

Entrance Aperture Definition

A brief design analysis, starting with the spectrometer entrance slit follows: The specified horizontal (perpendicular to the grating rulings) spatial resolution is 5 arc-sec or 2.42×10^{-5} radians. For a focal length of 212 cm, the entrance slit width is given by

$$2.42 \times 10^{-5} \times 212 = 5.14 \times 10^{-3} \text{ cm or } 51.4 \text{ } \mu\text{m}.$$

The corresponding slit width for an 8 arc-sec field of view in $8/5 \times 51.4 = 82.2 \text{ } \mu\text{m}$.

The widths for the "vertical" slits defined in Table 2.1-2 were calculated in a corresponding manner. The resultant designs for both horizontal and vertical slit foils are shown by GE drawing 47C231435, P1 and P2 respectively.

Entrance Aperture Mechanism

The initial objective of this study was to determine the changes required to the OSO-7 entrance aperture mechanism to incorporate the new fixed slit being developed under contract NAS5-23037, design a new movable slit to be compatible with the fixed slit, optimize the fixed slit (if required) and change the location of the reference point on the movable slit from the center of the spiral slit to the narrowest portion of the movable slit which is located on the optical centerline. During the initial stages of the study, assessment of the mission objectives suggested that the "spiral" slit on the movable element would not be required. With NASA/GSFC concurrence, it was deleted as part of the study program.

Incorporation of the fixed slit being developed under contract NAS5-23037 would provide two or more slit widths in the plane of dispersion of the diffraction grating. These slits are located along a common centerline on a foil which is positioned perpendicular to the optical centerline of the system. Since only one slit width can be placed on the system optical centerline, the adjacent slits will, therefore, be offset. This offset will be at least 50 arc seconds and is due to (1) a slit length which must accommodate a 60 arc second wide movable slit, (2) the end radii of the two adjacent slits, and (3) the bridge between the two adjacent slits.

To overcome the undesirable feature of operating with offset slits, GE investigated alternate designs which would provide the capability to vary both dimensions of the entrance aperture about the system optical centerline. The concept

was subsequently approved by NASA/GSFC and was included in the study program instrument configuration. The entrance aperture assembly is defined by GE drawing SK740925-1 and parts list A047D231437G1.

The approved concept incorporates two gear sectors which act as a support for the entrance aperture slits. These gear sectors are precisely positioned about the optical centerline and the slits are precisely placed on the gear sectors. Both gear sectors are movable and are driven by a single stepper motor through an appropriate gearhead. The aperture size of interest is obtained by commanding the motor a predetermined number of steps from the reference point which is located at the end of travel or from a known step position (see Section 3.2 for control circuits and a description of operation). Limit switches are provided to prevent over-travel in each direction.

Calculations were made to define the accuracy of the tracking of centerline of the "horizontal" slit relative to the optical centerline of the system. These calculations show that the accuracy of the tracking must be maintained to within ± 3 micrometers to maintain the position of a selected wavelength to within one step of its nominal position along the Rowland Circle. The calculations are included in Appendix B.

The full range of the mechanism required to obtain the apertures shown in Table 2.1-2 is 35.5° . This corresponds to 115 motor steps. Each slit position allows a ± 2.5 step tolerance (worst case) for rotational misalignment of the gear sectors and motor/gearhead backlash. The actual sum of tolerances and gear backlash equates to less than 1 motor step. The motor gearhead is the same one used for the OSO-7 entrance aperture mechanism and has a gear ratio of 60.75.

Exit Aperture Definition

The exit slits positions and widths have been calculated to meet the specified wavelength and resolution requirements as shown in Table 2.1-1. The results are shown in drawing 47D220794. The calculations are based on a grating position which is moved toward the center of the Rowland circle by 0.23 mm. This grating position results in optimum resolution and was arrived at by computerized ray tracing. The grating is not rotated.

A study was conducted to investigate the possibility of extending the wavelength range to include 9 nanometers (See Section 2.2 and Figure 2.2-1). It was decided to limit the travel to 12 nanoseconds because of interference problems at the shorter wavelength. A ray trace layout was prepared to show the relationship between the limiting rays for the 12 and 64 nanometer wavelengths, the six exit slit positions, the mask location and the 3 EUV detectors. The layout is defined by drawing SK750103-1 and is included as Figure 2.1-1. It proves that there is no crosstalk between detectors at any carriage or mask position, no interference of optical paths at the launch lock position with either mask position, and a considerable wavelength range overlap between detectors.

Because the spherical grating suffers from astigmatism, the height of the focused line varies according to Table 2.1-3.

Table 2.1-3
Image Height at Rowland Circle

Wavelength Nanometers	Line Height cm
0 order	1.18
12	1.53
64	2.35

The height of the exit slit is 1.9 cm (based on effective detector cathode height), therefore, some loss will occur at the longer wavelengths. Because the grating

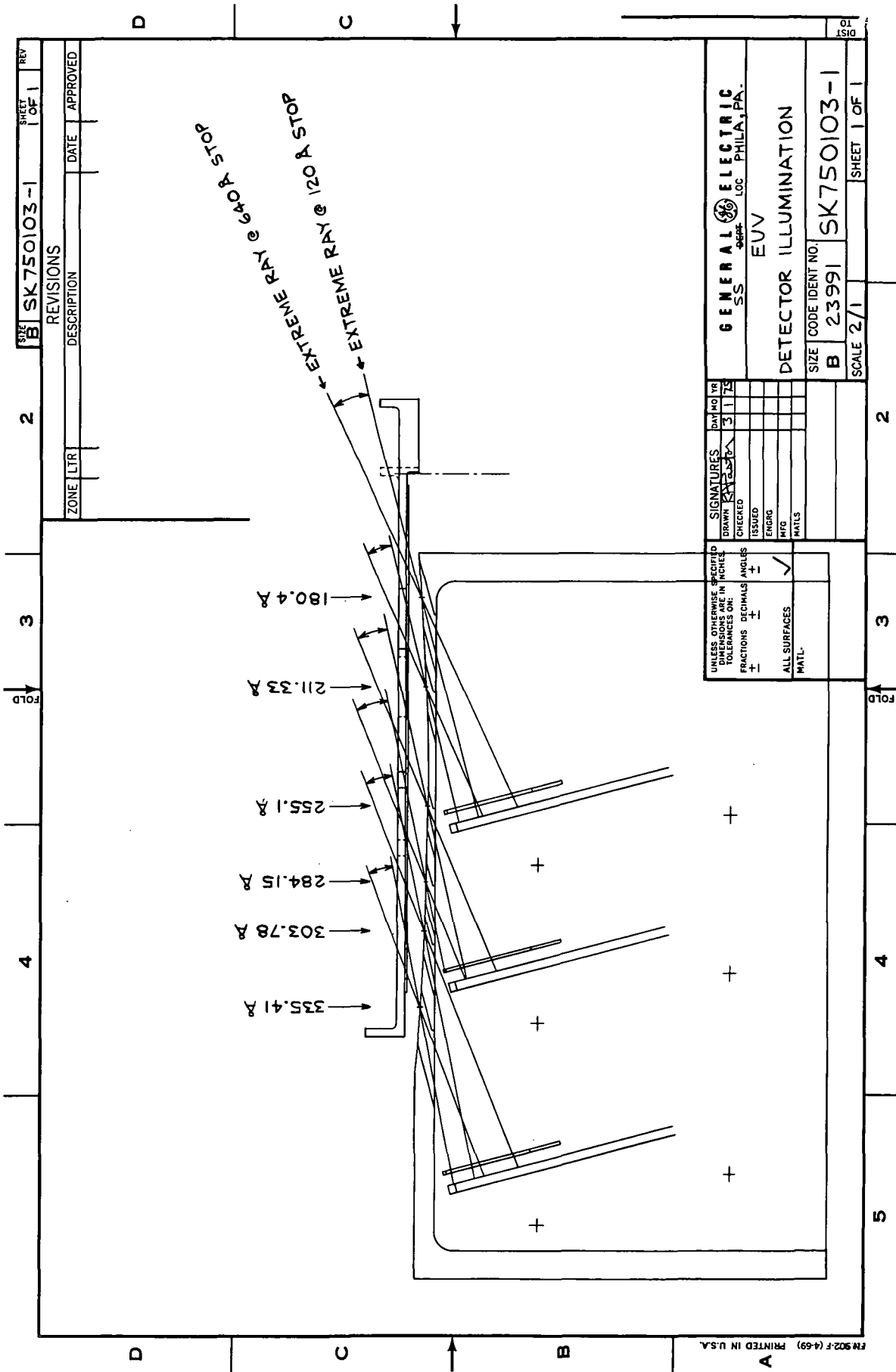


Figure 2.1-1. EUV Detector Illumination

is illuminated with a beam having an annular cross-section, a substantial fraction of beam intensity is concentrated at the extreme ends of the elongated image. The expected intensity loss will, therefore, be more severe than with uniform illumination. It may be advisable to use an ellipsoidal grating, as manufactured by Hitachi, which does not have any appreciable astigmatism and will maintain the image height to within the 1.9 cm aperture height.

Ion Trap

An ion trap located on the optical path between the grating and spectrometer exit slits was enlarged to accommodate the extended wavelength range without interference.

2.2 HYDROGEN-ALPHA SYSTEM STUDY

The objective of the study was to determine the best method to minimize, if not prevent, the occultation of the Hydrogen-Alpha optical path by the EUV mask motor due to the extension of the EUV spectral range.

Design Evaluations

Preliminary optical layouts revealed severe occultation of the H-Alpha optical path by the EUV carriage mask motor when the carriage was driven to the 9 nm position. The interference began at approximately the 12.4 nm position of the EUV carriage and continued to increase until it is totally occulted at approximately 11 nm. Also, the zero-order pick-off mirror for the H-Alpha system occulted the EUV radiation starting at approximately 15.9 nm and reducing the radiation to approximately 50% at 9 nm. These conditions are shown on SK740807-1 which is included as Figure 2.2-1.

To overcome these conditions, a new layout of the OSO-7 type spectrometer was prepared and was shown on 47J220792 Rev. A. This layout used the majority of

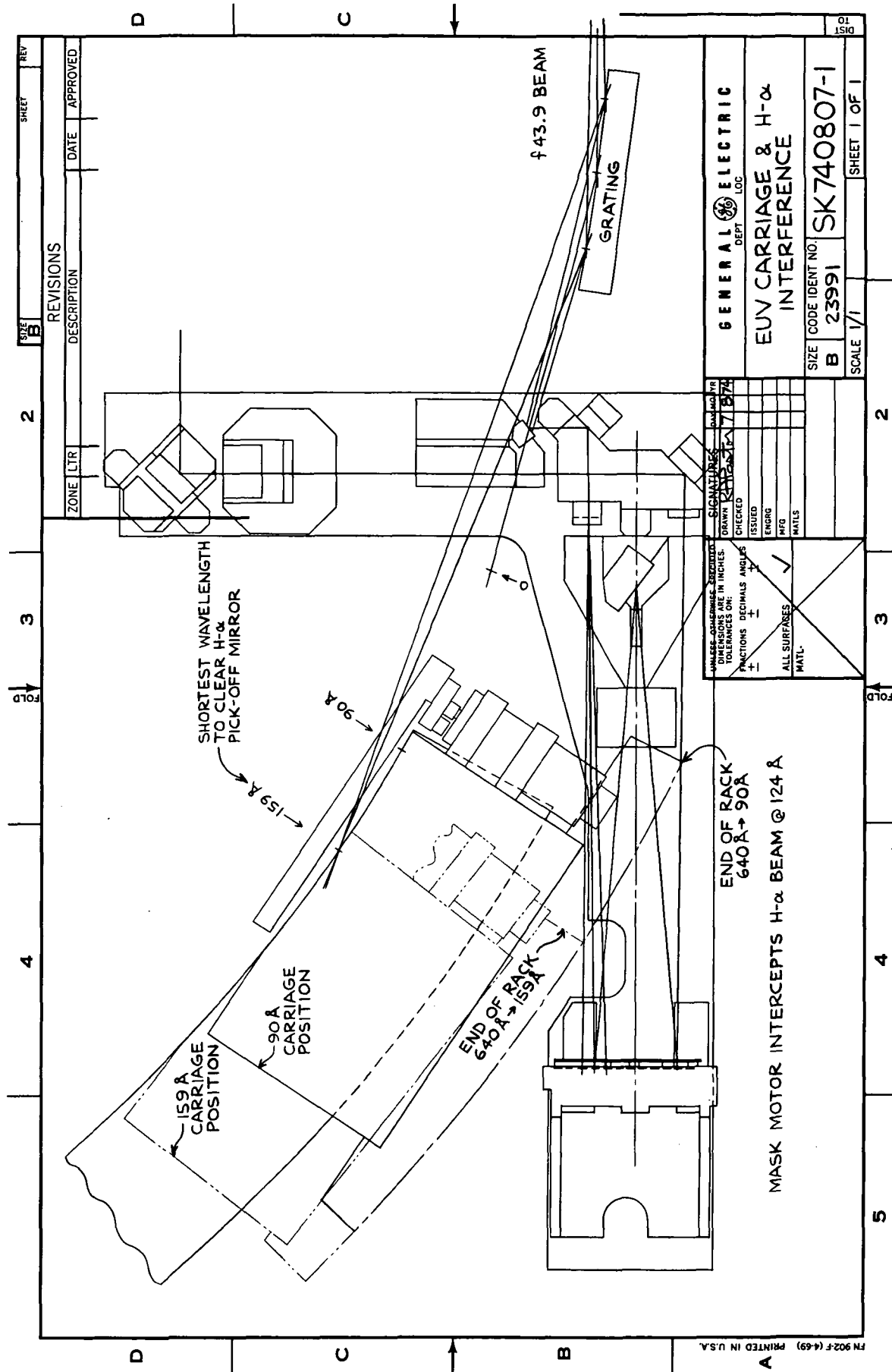


Figure 2.2-1. EUV Carriage and H-Alpha Interference

the OSO-7 components except for the use of new brackets and baseplate.

As the result of the meeting at NASA/GSFC on 5 September 1974, it was decided to limit the travel of the EUV carriage to the 12 nm wavelength and to use the proven OSO-7 H-Alpha design with minor modifications. The H-Alpha baseplate would be modified to provide clearance for the longer rack on the EUV carriage and the zero-order pick off mirror and bracket would be redesigned to eliminate the occultation at EUV wavelengths greater than 12 nm. This arrangement is shown on 47J220792 Rev B. Detail drawings were developed to define this configuration. This design was subsequently superceded by the Fabry-Perot etalon configuration described below.

Solid Fabry-Perot Etalon

The isolation of a narrow spectral region can be accomplished either by a dispersion method (spectrometer) or by non-dispersion methods such as interference filters. For spectral bandwidths of less than 0.2 nm, solid Fabry-Perot etalons usually have better spectral and thermal properties than do deposited type interference filters. Non-deposited solid spacer Fabry-Perot etalons are very stable, and are available with bandwidths to <0.05 nm and diameters to >7.6 cm. Air-spaced etalons can be made with similar properties, but are more sensitive to temperature, shock, and vibrations. If it is not necessary to transmit an image, then spectrometers can provide the desired spectral resolution; however, since they are also composed of a series of mechanically supported air-spaced components (mirrors, slits, grating), spectrometers are also more sensitive to shock and vibration than solid spacer etalons.

In summary, non-deposited solid spacer Fabry-Perot etalons have the basic advantages of small size and weight, and also a one-piece solid construction which

provides excellent resistance to shock and vibration. They do have the disadvantage of their bandpass center wavelength being somewhat temperature sensitive ($0.004 - 0.01 \text{ nm}/^\circ\text{C}$) although less so than is the case for air spaced etalons ($0.1 \text{ nm}/^\circ\text{C}$) or deposited interference filters ($0.02 \text{ nm}/^\circ\text{C}$). Thus, the use of a solid etalon requires modest thermal control.

With these solid etalon characteristics in mind, the general characteristics of the OSO H-Alpha spectroheliograph were examined while assuming the use of a relatively low cost commercially available solid spacer Fabry-Perot etalon as the H-Alpha line isolating device.

The assumed geometry and optics include, in order, the use of a convex cylindrical mirror to deflect and collimate (in the plane of dispersion) the zero order radiation from the EUV grating, a cylindrical lens to complete the collimation of the zero order rays which then fall on the etalon, a condensing lens located after the etalon, and finally a photomultiplier tube (PMT) detector.

The convex cylindrical collimating mirror and the convex cylindrical collimating lens are such as to focus horizontally on the zero order virtual slit image and to focus vertically on the telescope slit, respectively. If the convex cylindrical mirror has an effective focal length (for 45° angle of incidence) of -4.8 cm , and if the cylindrical lens has a focal length of $+26 \text{ cm}$, then the collimated beam would have a cross-section size of 1.2 cm high by 0.2 cm wide. In this case, if we also assume the use of an $8 \text{ arc-sec} \times 60 \text{ arc-sec}$ telescope slit (long dimension is vertical), then the collimated light beam will have a maximum angular deviation from its optical axis of 0.05° horizontal and 0.07° vertical (beam half-angle), respectively. These small maximum deviations from parallelism will result in $<0.01 \text{ nm}$ variation in etalon transmitted wavelength.

Let us now calculate the detector output current (I_S) given a realistic set of optical and electrical conditions as well as the use of a relatively low cost commercially available solid spacer Fabry-Perot etalon (Carson Astronomical Instruments Inc. "SkySpear" filter). The PMT photocathode current (I_S/G) is then

$$I_S/G = B_{H\alpha} A E_t F_{S1} E_g E_o E_f \cdot \Delta\lambda \cdot S_k \text{ amps}$$

where

$$F_{S1} = S_1 S_2 K^2 R_e^2 / (\pi r_s^2) = 3.45 \times 10^{-7} S_1 S_2$$

The symbol definitions and their assumed values are as follows:

G	= PMT gain (dynode amplification)
$B_{H\alpha}$	= solar spectral irradiance at the center of the Balmer $H\alpha$ line where $0.1 B(\text{sun}) \leq B_{H\alpha} \leq 1.3 B(\text{sun})$
$B(\text{sun})$	= solar spectral irradiance near the $H\alpha$ line = $0.1494 \text{ W cm}^{-2} \mu^{-1}$
A	= spectroheliograph telescope area = 35.00 cm^2
E_t	= efficiency ("transmittance") of spectroheliograph telescope = 0.128
F_{S1}	= fraction of sun's disc included in telescope fov as defined by the slits
E_g	= reflectivity of $H\alpha$ light by the spectroheliograph grating into its zero order image = 0.9.
E_o	= net efficiency of all optics not otherwise specified, = 1 mirror (Al + SiO) and 2 lenses (MgF ₂ coated) = $0.85 \times (0.985)^4 = .80$
E_f	= etalon peak transmittance = 0.03
$\Delta\lambda$	= etalon FWHH bandpass = $0.7A = 7 \times 10^{-5} \mu$
S_k	= PMT cathode sensitivity at the $H\alpha$ wavelength = 0.026 amps/watt for EMR #510E-01-13
S_1 & S_2	= slit width and height in arc seconds = 5 arc-sec each
K	= arc seconds/radian conversion factor
R_e	= earth's distance from sun
r_s	= sun's radius

The gold coated grating was assumed to have such a high zero order efficiency at 656.5 nm ($E_g = 0.9$) because gold has a reflectivity of over 0.95 at the $H\alpha$ wavelength and because a grating made for the first order in the EUV (<100 nm) will act mostly as a mirror for visible and longer wavelengths, strongly concentrating those wavelengths into the zero order.

Geometric calculations show the average incidence angle of light on the compound telescope's two mirrors to be 10.67° . This grazing incidence angle on uncoated fused quartz yields a calculated single surface reflectance of 0.3572 at 656.5 nm. Thus the telescope average total reflectance or overall "transmittance" (E_t) = $(0.3572)^2 = 0.1276$.

Upon substituting all the above conditions into the equations, we find that for a 5×5 arc-sec fov, $I_s/G = 2.26 \times 10^{-14}$ amps to 2.9×10^{-13} amps depending on the value used for $B_{H\alpha}$. This range of PMT photocathode signal current should be compared with the manufacturer-stated PMT dark current (I_d) which yields a typical cathode $I_d/G = 1.5 \times 10^{-16}$ amps at 20°C . Since I_d will double for each 5°C rise in cathode temperature, we obtain $I_d/G = 3 \times 10^{-16}$ amps at 25°C which allows us to calculate the minimum signal/dark current ratio of 75.3. Thus

$$I_s/I_d > 75.$$

Using the OSO-7 H-Alpha data integration time of 142 m sec (and thus an effective signal bandwidth of 2.5 Hz), the above PMT currents permit calculation of the minimum signal-to-noise ratio (S/N) from the sum of minimum I_s/G plus maximum I_d/G . If we assume the noise current to be primarily shot noise rms current from the PMT photocathode ($I(\text{shot})/G$), then we calculate that

$$S/N = I_s/I(\text{shot}) \geq 169$$

If we assume the PMT output current (I_s) measuring integrating capacitor to again be 10 nfd and to again be shorted out (and called one "count") when its potential

increases to 1mV, we can then calculate the time/count for each experimental condition. Finally, given the same 0.142 second counting period per H α measurement, we can also calculate the total counts per H α measurement. Some results from these types of calculations are shown in the following table given the conditions listed earlier (including a 5 x 5 arc-sec fov):

PMT Applied Voltage PMT Gain, G	Volts ---	2450 10 ⁶		1750 10 ⁵	
Rel. line int., B _{Hα} /B(sun)	--	0.1	1.3	0.1	1.3
PMT output, I _s	na	22.6	295	2.26	29.5
Time/count	ms	.442	.034	4.42	.339
Counts/.142 sec	--	321	4185	32.1	419

The count levels can be further varied by using a different size fov (different slits), by using different PMT gains, by changing the integrating measurement capacitor to a different value, or by changing the count period length. Of course, signal levels can always be reduced through addition of a neutral density filter in front of the PMT, or increased through use of a solid etalon with better peak transmittance (more expensive) or wider bandpass than assumed.

As indicated earlier, because the solid etalon center wavelength is somewhat sensitive to temperature, it is necessary to provide a constant temperature environment or oven with temperature held constant within $\pm 0.5^{\circ}\text{C}$ or less. Although the relatively low cost solid etalon assumed for the above spectroheliograph calculations is supplied by the manufacturer complete with blocking filters and already in an oven, the normally supplied oven is not designed for satellite use and also draws too much power. Given the 15 $^{\circ}$ -25 $^{\circ}\text{C}$ spectroheliograph internal environment, a low oven temperature (at about 30 $^{\circ}\text{C}$) will permit all of the necessary thermal control consistent with keeping the temperature differential small so as

to reduce power consumption. Thus assuming the use of a 1 inch diameter solid etalon plus blocking filters, a relatively low oven temperature, and careful insulation, it should be possible to thermally control the etalon with 100 mW of heater power (duty cycle of 25%), and 200 mw of control electronics power.

In conclusion, it would appear that the use of a solid Fabry-Perot etalon as the wavelength-selecting device in the H α spectroheliograph is not only practical, but should result in much more spectral stability (to shock and vibration) and greater ease of initial adjustment than was true for the Ebert monochromator used in the previous OSO spectroheliographs.

The detailed design of the Fabry-Perot Etalon H-Alpha system was not included as part of the study program. A preliminary design, however, was conducted, and the results are shown on 47J220792 Rev. C.

2.3 INSTRUMENT HOUSING

2.3.1 REQUIREMENTS

The purpose of this portion of the study was to prepare a layout for the new instrument housing to accommodate the new EUV telescope, new X-Ray collimator, extended travel of the EUV carriage and a revised H-Alpha optical path. The mechanical design would provide for the alignment of the optical axes of the telescope and collimator to within 5 arc seconds and, after vibration to OSO-7 specifications or while in an OSO-7 orbital environment, maintain the recorded alignment to within 3 arc seconds. The material of the housing and other structural parts were to be assumed to be beryllium. The dynamic and thermal analyses associated with the design of the housing would be conducted by NASA/GSFC.

2.3.2 HOUSING DESIGN

A layout of the instrument housing was prepared and is defined by SK741122-1. The overall size of the housing is 133.35 cm long, 14.58 cm wide, and 30.48 cm high (52.50 x 5.74 x 12.00 inches, respectively). Appropriate openings are provided for the telescope and X-Ray collimator. Three openings are provided; two to assist in the alignment of the EUV system and one to act as a vent. Two purge ports and a hole for the launch lock pin will be added along with the mechanical and electrical interface provisions when the latter items are defined.

The baseplate is 2.54 cm (1.0 in) thick. This thickness is arbitrary and may be reduced in accordance with the results of the thermal and dynamic analyses and the definition of the mechanical interface.

The inside surface of the baseplate has been located relative to the EUV telescope and X-Ray collimator optical center lines to permit the use of OSO-7 hardware without spacers or adapters.

The methods to be used to mount and align the EUV telescope and X-Ray Collimator will be the same as employed for OSO-7. These methods will result in an initial alignment of their respective optical centerlines to within 5 arc seconds of each other. The thermal and dynamic analyses to be conducted by NASA/GSFC will provide data which will be used to evaluate the ability of the design to maintain the "as-aligned" condition to within 3 arc seconds when the instrument is exposed to OSO-7 level environments.

Due to the increased length of the X-Ray Collimator, it will be necessary to install the collimator through the opening in the front face of the instrument and through the forward bulkhead. A baffle plate will be provided to reduce the size of the opening in the front face to an appropriate size after the collimator is installed and aligned. Provisions will be provided on the baffle plate to assist in the final balancing of the two X-Ray systems.

An advanced parts list was prepared for the instrument housing and is defined by A047J231443G1.

2.4 INSTRUMENT ASSEMBLY

2.4.1 REQUIREMENTS

This portion of the study was directed toward the definition of an instrument assembly which incorporates the improvements developed during the study program. The instrument assembly drawing was to be in the form of a general arrangement drawing.

All major component and hardware items were to be shown and identified by a unique drawing number. Existing OSO-7 drawings were to be used where ever possible and modified parts would be used where economically feasible. Modified and new parts would be defined by modified OSO-7 drawings, new drawings, lay-

outs, or sketches as appropriate. All outstanding Alteration Notices (ANs) would be incorporated on OSO-7 drawings used to define the new assembly. Electronic drawings would not be revised to incorporate outstanding ANs as part of the study program.

2.4.2 GENERAL ARRANGEMENT DRAWING

General Arrangement Drawing 27J231440 was developed to show the placement of the major component and hardware items within the new instrument. The major items have been identified by name and part number on the drawing. A separate parts list (47J231440G1) has been provided to identify other significant hardware items at the instrument assembly level. Assembly hardware such as fasteners, adhesives, etc. are not included on either the drawing or parts list.

Significant features which are not shown on the drawing are the mechanical and electrical interfaces to the spacecraft and the location and packaging of the control and data processing electronics. The control and data processing electronics will be packaged separately and located remotely from the instrument assembly. The finalization of these items are outside the scope of the study program.

2.4.3 SUBASSEMBLY AND COMPONENT DRAWINGS

Drawings have been prepared for each subassembly and special component (part) which could be fully designed under the scope of the study program. OSO-7 drawings which are used to define the new instrument configuration have been updated to incorporate all outstanding Alteration Notices (except electronics drawings).

Parts lists have been generated for each subassembly. The parts list for the top assembly is defined by parts list 47J231440G1. All parts lists are either

listed here or at a lower tier. The parts lists for the electronics have been updated to incorporate all outstanding Alteration Notices.

Subassemblies which require additional definition are listed in Table 2.4-1. Advanced (A0) parts lists have been prepared for each of these assemblies and are included in the definition of the new instrument. Drawings depicting these subassemblies were not prepared as part of the study program.

Table 2.4-1
Subassemblies Requiring Additional Design Activity

Subassembly	Identification	Information Required
Box Assembly	47E231443G2	Interface, Dynamic & Thermal Analyses
EUV Carriage Assembly	47E217398G2	HVPS, Wiring
Ent. Aperture Assembly	47D231437G1	Thermal Analysis
H-Alpha Filter Assy.	47D231438G1	Detail Design
H-Alpha Filter/Heater Assembly	47D231439G1	Detail Design, Thermal Analysis
H-Alpha Lens Assembly	47C231441G1/G2	Detail Design

Several instrument components also will require additional design activity to complete the definition of the instrument. These components are listed in Table 2.4-2.

Table 2.4-2

Components Requiring Additional Design Activity

Component	Activity
Thermal Shields	Thermal Analysis
High Voltage Power Supplies	Identification of Supplier Interface
Flex Circuits & Terminations	Electrical & Mechanical Interface
Instrument Baffle Plates	Box Assembly Design

2.4.4 DRAWING TREE

A drawing tree, GE Drawing 27J231446, was prepared to display the major components and hardware items contained in the new instrument.

2.5 NEW PARTS AND MATERIALS

This portion of the study was directed toward the identification of parts and materials which are different from OSO-7 parts and materials to the extent that they do not fall within the framework of the OSO-7 approved parts and materials list.

Parts and materials which will require NASA/GSFC approval are listed in Table 2.5-1. The balance of the parts and materials used in the definition of the instrument are either the same as OSO-7 or are similar to the extent that they do not require further approval. Electronic parts are covered separately in Section 3.8.

Table 2.5-1
New Parts and Materials

Description	Part Number
H-Alpha Filter (Etalon)	(Later)
H-Alpha Heater	(Later)
Photomultiplier Tube	EMR 510E-01-13 *
Gear	47C217575P2

*Electro-Mechanical Research
Part Number

2.6 PARTS COMMON TO OSO-7

2.6.1 REQUIREMENTS

This portion of the study was directed toward the identification of OSO-7 parts (except electronic parts) which would be usable in the instrument configuration defined during the study program. Parts which can effectively be modified will also be identified.

2.6.2 IDENTIFICATION OF PARTS

Drawing tree, GE Drawing 47J231446, was prepared to display all of the components and major hardware items contained in the new instrument configuration. The drawing tree also displays information indicating whether each part is the same as OSO-7, a modified OSO-7 part, or a new part. The drawings identified on the drawing tree contain the necessary information required to modify the OSO-7 parts which can be effectively modified. The drawing tree is included as Figure 2.6-1.

2.6.3 SHELF-LIFE LIMITED COMPONENTS

In some cases, residual components from the OSO-7 program contain items which are subject to shelf-life restrictions. These components are those which contain O-rings, pyrotechnics, and are lubricated with the LUBCO 905 process.

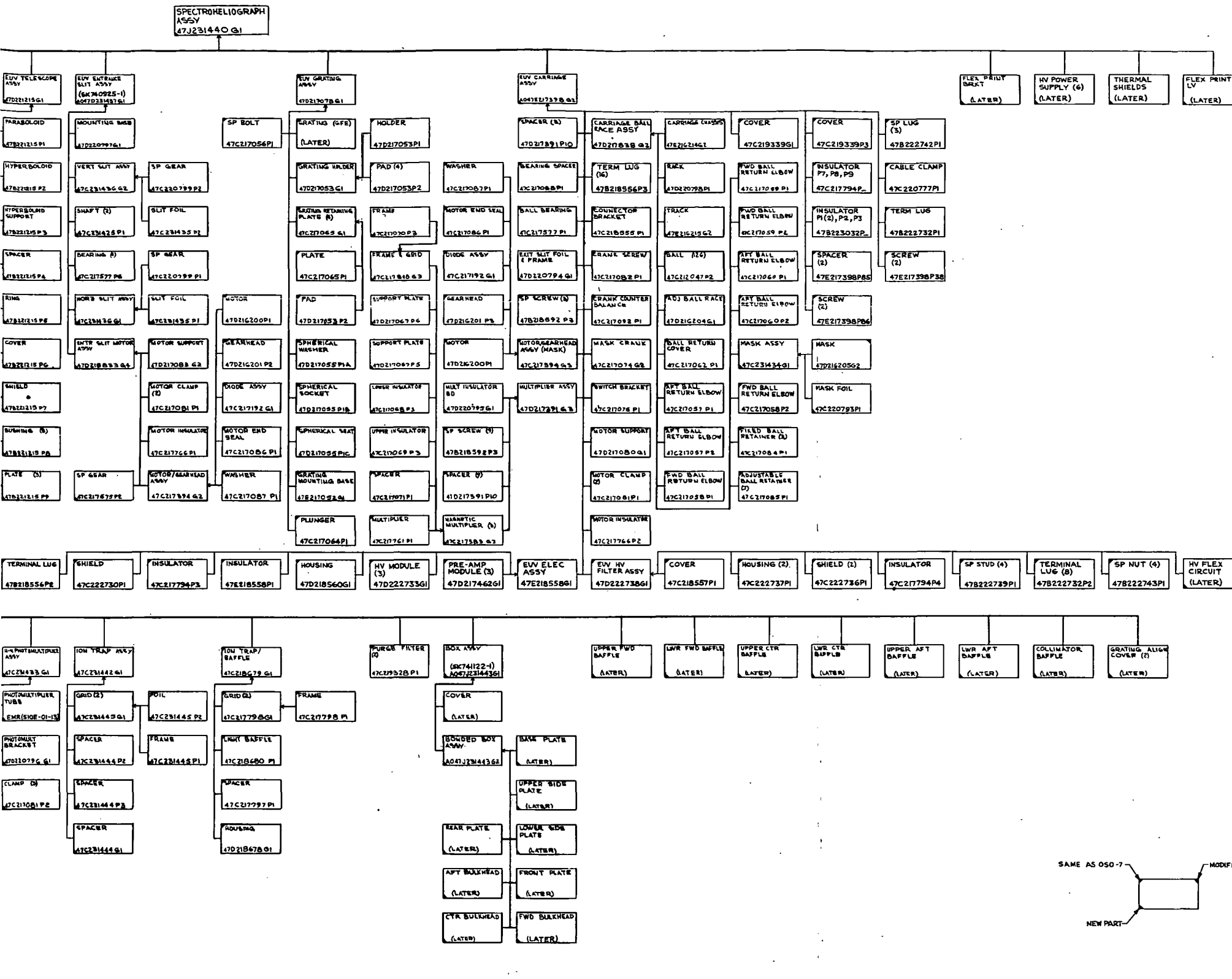
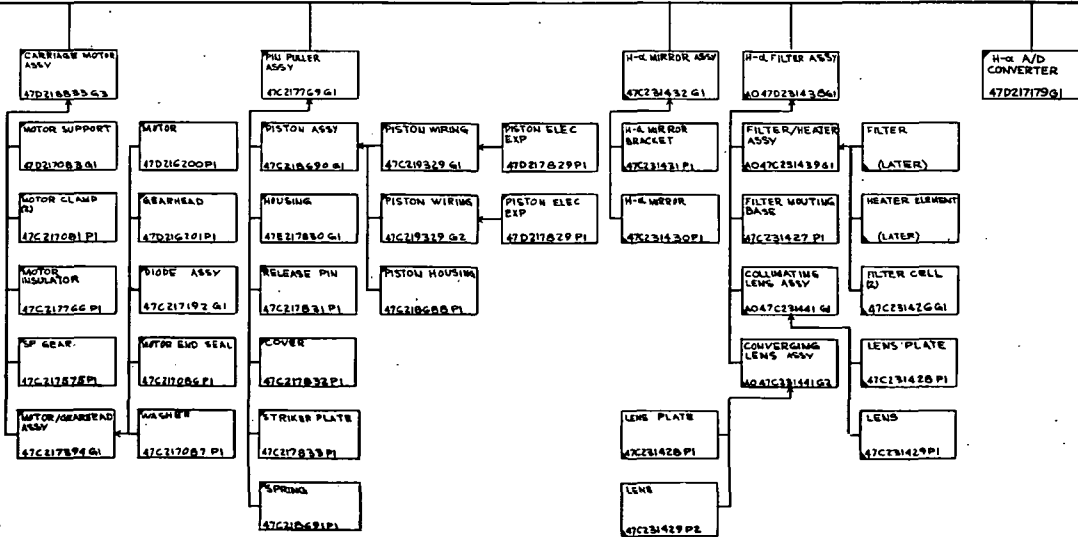
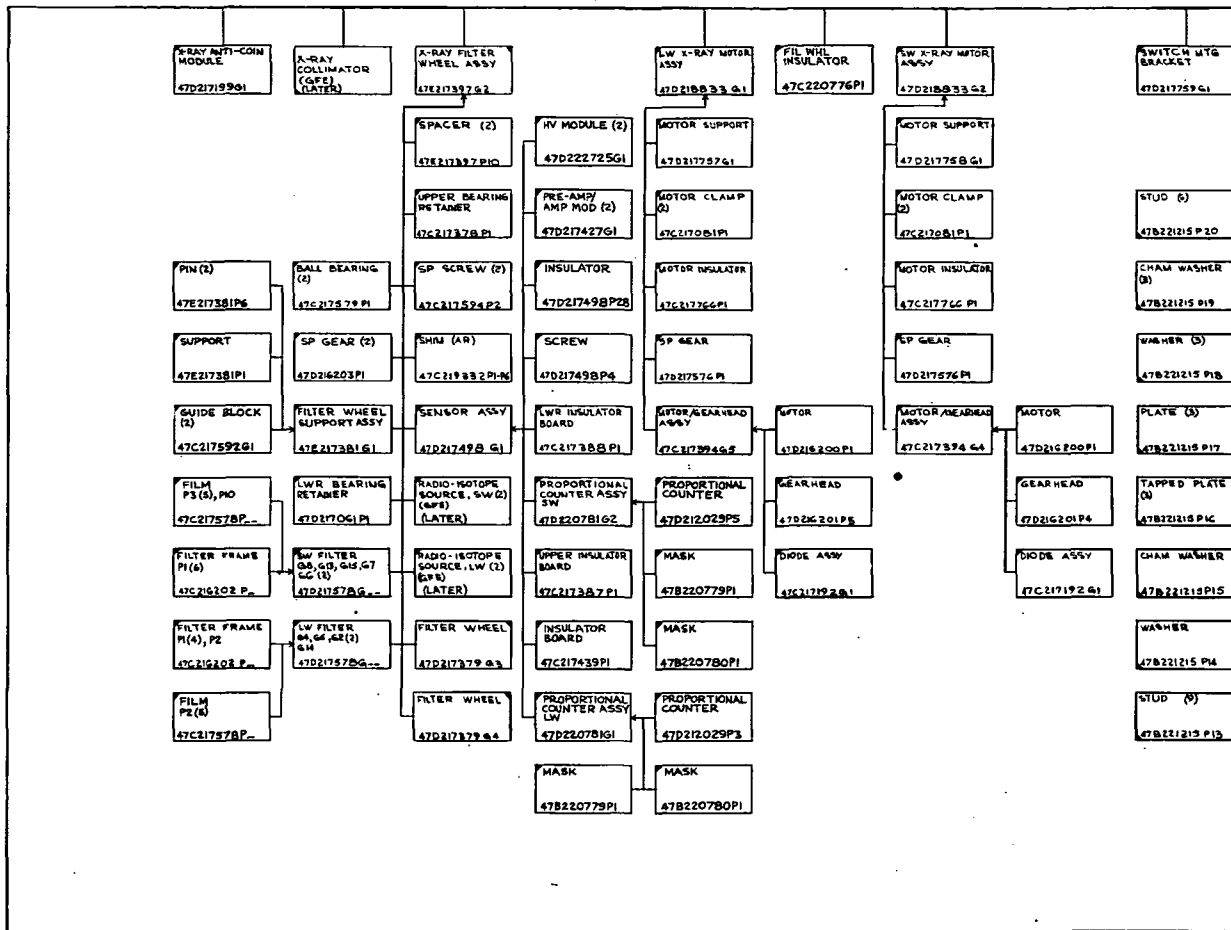


Figure 2.6-1. Drawing Tree



These components are listed in Table 2.6-1 and will require refurbishment before use in the new instrument assembly.

Table 2.6-1
Shelf Life Limited Components

Component	OSO-7 Part Number	Restriction
Motor/Gearhead	47C217394G1	Lubrication, O-Ring
Motor/Gearhead	47C217394G2	Lubrication, O-Ring
Motor/Gearhead	47C217394G3	Lubrication, O-Ring
Motor/Gearhead	47C217394G4	Lubrication
Motor/Gearhead	47C217394G5	Lubrication
Ball Bearing	47C217577P1	Lubrication
Ball Bearing	47C217579P1	Lubrication
Gear	47C217575P1	Lubrication
Gear	47D217576P1	Lubrication
Gear	47D216203P1	Lubrication
Adjustable Ball Race	47D216204G1	Lubrication
Ball Return Cover	47C217062P1	Lubrication
Ball Return Elbow	47C217057P1	Lubrication
Ball Return Elbow	47C217057P2	Lubrication
Ball Return Elbow	47C217058P1	Lubrication
Ball Return Elbow	47C217058P2	Lubrication
Ball Return Elbow	47C217059P1	Lubrication
Ball Return Elbow	47C217059P2	Lubrication
Ball Return Elbow	47C217060P1	Lubrication
Ball Return Elbow	47C217060P2	Lubrication
Carriage Chassis	47E216214G1*(G2)	Lubrication
Exit Slit Mask	47D216205G1*(G2)	Lubrication
Release Pin	47C217831P1	Lubrication
Piston Assembly	47C218690G1	Pyrotechnics

* Modification to G2 required for use in new instrument configuration

SECTION 3

COMMAND, CONTROL, AND DATA PROCESSING STUDIES

3.1 GENERAL REQUIREMENTS

This general class of studies relates to the instrument electronics and is directed toward the expanded operational capability of the instrument. The output of these studies will be presented in schematic/logic diagram format with a description of how the circuitry operates. A power summary, electronics parts list, command list, and telemetry list will also be provided as part of the study.

3.2 CONTROL OF EUV ENTRANCE APERTURE MECHANISM

The initial study requirement was to incorporate changes to the OSO-7 logic to provide greater flexibility in the operation of the OSO-7 type entrance aperture mechanism. The study requirements were modified with the adoption of the new entrance aperture mechanism described in Section 2.1. The new requirements included the capability to command the mechanism to any aperture size from any position and to provide a reference position at one end of travel of the mechanism. A means of reading out the entrance aperture mechanism position (aperture size) was also required.

3.2.1 MODES OF OPERATION

The entrance aperture mechanism has four modes of operation. These modes of operation are described below.

Advance to a Selected Step Number (Aperture Size). Upon command, the mechanism will advance to the last step number entered into the control register at 50 steps per second. The step number is measured from the zero or reference point which is located at the smallest aperture position. While in this mode,

changing the step number in the control register will cause the mechanism to automatically move to the new step position and stop.

Return to Reference. Upon command, the mechanism will return to the reference point (smallest aperture) at 50 steps per second.

Scan Apertures. Upon command, the mechanism will begin to scan the apertures at 6.25 steps per second and will continue to scan between the two extremes in travel until commanded to stop.

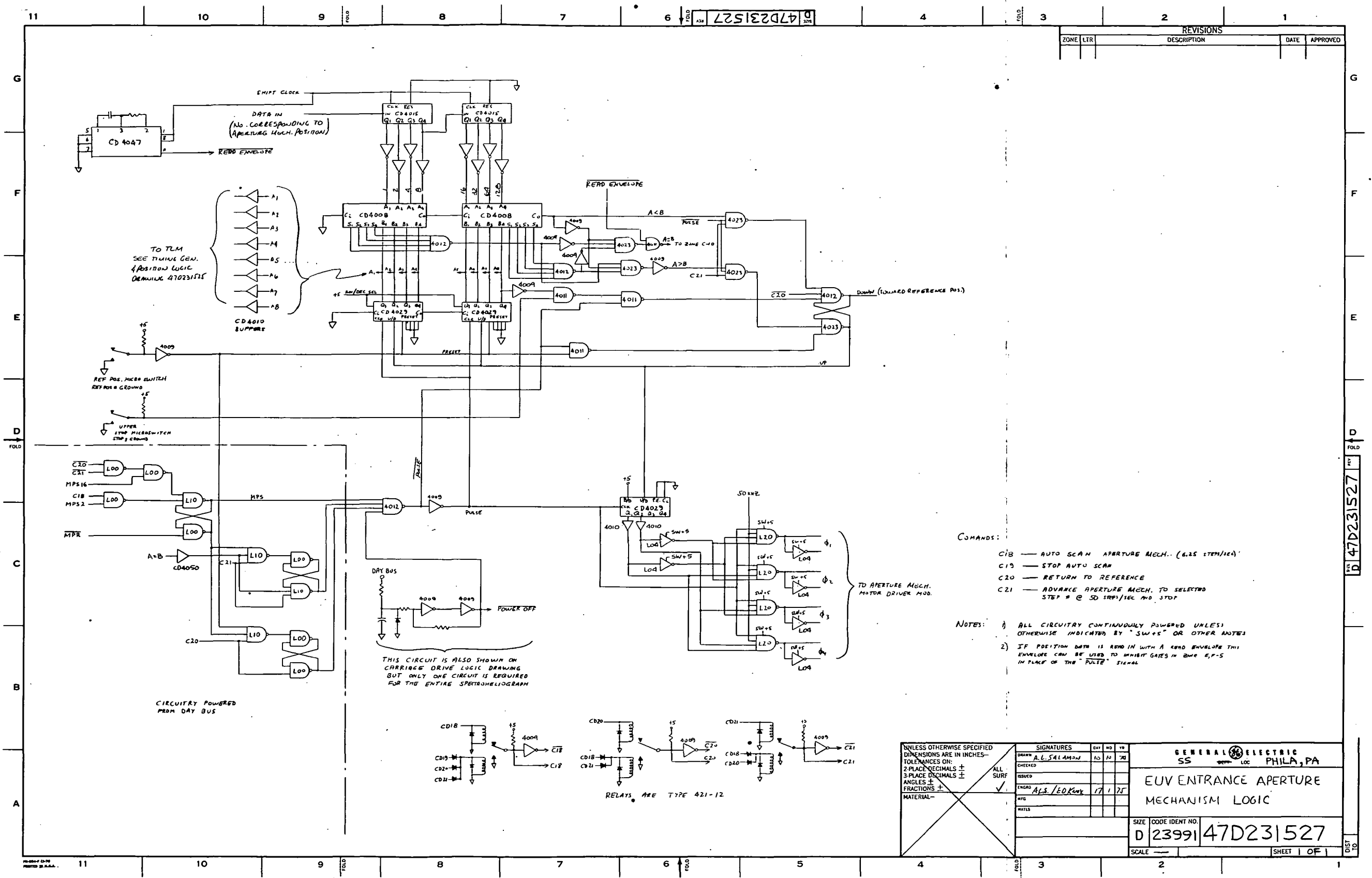
Stop Scan of Apertures. Upon command, the entrance aperture mechanism will stop the scan mode of operation. This command will not effect either the "Advance to Selected Step Number" or "Return to Reference" mode.

3.2.2 CIRCUIT DESCRIPTION - EUV ENTRANCE APERTURE MECHANISM

The logic receives commands from the spacecraft and provides the proper sequence of motor pulse signals to the motor driver modules to execute the motions called for by the commands. A detailed description of the logic by operating modes is given below. Drawing 47D231527 is referenced by zones in the description and is included as Figure 3.2-1.

Scan Apertures. Command pulse CD18 from the spacecraft picks a latching relay to produce a HI state on signal C18 (and a LO state on Signal $\overline{C18}$). This command pulse also resets the other command relays to deactivate the previous mode of operation.

In zone D11, signal C18 enables the 6.25 pps signal (MPS-2) from the original OSO-7 logic to step the motor at 6.25 steps per second. The direction of motion is the same as the last direction in the previous mode unless the previous mode has been "Return to Reference" in which case the mechanism is already



REVISIONS				
ZONE	LTR	DESCRIPTION	DATE	APPROVED

COMMANDS:

- C18 — AUTO SCAN APERTURE MECH. (6.15 STEPS/SEC)
- C19 — STOP AUTO SCAN
- C20 — RETURN TO REFERENCE
- C21 — ADVANCE APERTURE MECH. TO SELECTED STEP # @ 50 SRP/SEC AND STOP

NOTES:

- 1) ALL CIRCUITRY CONTINUOUSLY POWERED UNLESS OTHERWISE INDICATED BY "SW+S" OR OTHER ANNOT.
- 2) IF POSITION DATA IS READ IN WITH A READ ENVELOPE THIS ENVELOPE CAN BE USED TO INHIBIT GATES IN QMC E.P.-5 IN PLACE OF THE "PULSE" SIGNAL

UNLESS OTHERWISE SPECIFIED DIMENSIONS ARE IN INCHES— TOLERANCES ON: 2-PLACE DECIMALS ± 3-PLACE DECIMALS ± ANGLES ± FRACTIONS ± MATERIAL—	SIGNATURES		DATE	BY	GENERAL ELECTRIC SS PHILA, PA EUV ENTRANCE APERTURE MECHANISM LOGIC
	DRAWN: A.L. SALAMON		10	70	
	CHECKED:				
	ISSUED:				
ENGRS: ALS/EDK		17	75		SIZE: D 23991 CODE IDENT NO: 47D231527
MATERIAL:					SCALE: SHEET 1 OF 1

Figure 3.2-1. EUV Entrance Aperture Mechanism Logic

at position 0 and will move toward the larger apertures. If the mechanism is started toward the UP direction, it will move away from the reference position until 128 pulses have been accumulated by the CD4029 up/down counters. When the bit corresponding to 128 goes HI, it is gated through a CD4011 gate (Zone E-6) to set the direction flip-flop to the DOWN state and on the next pulse, the direction of motion will reverse. The "128" line is ANDed with the $\overline{\text{PULSE}}$ signal to prevent changing directions during a pulse; this insures that the last pulse is completed before direction is changed. When the direction flip-flop is in the UP state, it causes both sets of up/down counters to count up.

One up/down counter (Zone E-8) counts motor pulses and keeps track of the position of the mechanism; the second up/down counter at Zone D-6 sequences the phasing of the motor pulses so that the motor will move in the up or down direction as a function of the order in which \emptyset_1 through \emptyset_4 are selected. By telemetering the count in the first up/down counter, the position of the mechanism is always known.

A count of 0 corresponds to the reference position at the center of the smallest aperture and a count of 128 corresponds to the end of the slit farthest from reference position. A microswitch at the reference position clears the up/down counter to 0 whenever the mechanism is at that position; this periodically corrects the counter in case it has miscounted due to noise spikes and is the only true position feedback in this servo system. Tripping the microswitch also sets the direction flip-flop to the UP state as soon as the motor pulse has stopped---this gating is done in CD4011 gate in Zone E-7. Since the MPS pulses are not stopped in this mode, the mechanism will keep moving between the "0" and "128" count positions changing direction whenever it reaches these points. A microswitch just past the "128" position does not update the count-

er, but will set the direction flip-flop to the DOWN state in case the counter circuitry should fail.

Stop Scan of Apertures. This command (CD19) resets the "Scan Apertures" command relay and, upon its receipt, causes the aperture mechanism motion to stop. This command effects the "Scan Apertures" function only.

Return to Reference. Command pulse CD20 picks a latching relay to cause signal C20 to go HI and also resets all other command relays thereby terminating the previous mode. Signal $\overline{C20}$ going LO sets the direction flip-flop to the DOWN state (Zone E-5) and also enables MPS16 (Zone D-11) which is the 50 pps signal from the existing OSO-7 logic. Thus the mechanism will turn toward the 0 count position at 50 steps per second. When the microswitch is tripped at the 0 count position (reference position), the inhibit flip-flop in Zone B9 is set to the inhibit state and prevents further pulses from getting through thus stopping the mechanism (pulses are inhibited in CD4012 gate in Zone C-8).

The \overline{MPR} signal is ANDed with the microswitch signal (and the C20 signal) in the gate at Zone B-10 to prevent shutting off the pulse before it is finished; thus the pulse which drives the mechanism to the reference is allowed to be completed before further pulses are inhibited. The inhibit flip-flop is reset when C20 goes low i.e. when a new mode is commanded and the C20 command relay is reset. Thus the mechanism will remain in the reference position until either the "Scan Apertures" or "Advance to Selected Step Number" command is received.

Advance to Selected Step Number. Command pulse CD21 from the spacecraft picks a latching relay causing C21 to go HI and also terminating the previous mode by resetting all other command relays. Prior to sending this command, the register in Zone G-8 should be loaded with the desired step number since the

mechanism will go to the last number stored in this register. The loading is done by two signals from the spacecraft: one is the data line containing the number corresponding to the desired position, and the other a shift pulse line to shift in this number (see Section 3.13).

A digital magnitude comparator composed of the CD4008 adders and associated gates and inverters in Zone F-7, -8, -9 compares the desired position number in the register to the number in the up/down counter (actual mechanism position) and produces a HI on one of three lines: $A > B$, $A < B$ or $A = B$ (where "A" is the desired number and "B" is the present position number). When enabled by the C21 mode signal, " $A > B$ " sets the direction flip-flop to the "UP" state and " $A < B$ " sets the direction flip-flop to the DOWN state causing the motor to step in the direction to reduce the difference between A and B. When $A = B$ goes HI, it sets an inhibit flip-flop in Zone C-10 inhibiting further pulses. ($A = B$ is ANDed with \overline{MPS} to prevent inhibiting until that pulse has finished.) The inhibit flip-flop is reset when a new mode is commanded (C21 goes LO) or when $A = B$ goes LO, which would happen if a new number were read into the register.

Other Features. When the Day Bus is turned off, the Power Off signal goes LO and inhibits all further pulses thus insuring that all critical circuitry remains undisturbed and in the same state as before power turn off; the critical circuitry is continually powered. At power turn on, the power off signal returns HI with a delay insuring that all turn on transients have died out before allowing normal operation. The signal which generates power off is located in Zone B/C-8 and the inhibiting is done in the 4012 gate at Zone C-8.

The "one shot" in Zone F-11 produces an inhibit pulse during the time when a new number is read into the shift register. This inhibit pulse prevents the

generation of false pulses on the clock line which, in turn, would cause errors in the position counter. This inhibit pulse insures that signal "A=B" remains HI during the read-in period by forcing the output of the 4011 gate in Zone F-6 HI.

Interfaces. Inputs from existing OSO-7 logic:

MPS2	6.25 pps pulses
MPS 16	50 pps pulses
$\overline{\text{MPR}}$	resets flip-flop which produces MPS signal
50 KHZ	to modulate motor commands

Outputs to existing OSO-7 circuits:

\emptyset_1	} to motor driver modules (signals same as for OSO-7 and will interface directly with present OSO-7 modules)
\emptyset_2	
\emptyset_3	
\emptyset_4	

Inputs from spacecraft:

CD18	} Command pulses which select operating modes (same spec as for OSO-7)
CD19	
CD20	
CD21	
DATA IN	number representing desired position
SHIFT PULSES	to shift in above number

3.3 CONTROL OF EUV CARRIAGE

This portion of the study was directed toward improving the operational capability of the EUV carriage. The study was to develop a method to command the carriage to a precise step number (wavelength position) without the execution of a timed command as used for OSO-7. It was also desired to introduce the capability to scan over a portion of the total travel of the carriage and to read-out the exact position of the carriage. The study would preserve the balance of the operational features common to OSO-7.

3.3.1 MODES OF OPERATION

The EUV carriage has six modes of operation. These modes of operation are described below.

Continuous Scan at 12.5 Steps per Second. Upon command, the EUV carriage will scan the full spectral range at 12.5 steps per second and continue to scan between the limits until another command is given. The scan will start toward the long wavelength end.

Continuous Scan at 6.25 Steps per Second. Upon command, the EUV carriage will scan the full spectral range at 6.25 steps per second and will continue to scan between the limits until another command is given. The scan will start toward the long wavelength end.

Slew to Long Wavelength End and Stop. Upon command, the EUV carriage will slew to the long wavelength end at 50 steps per second and stop.

Slew to Short Wavelength End and Stop. Upon command, the EUV carriage will slew to the short wavelength end at 50 steps per second, and stop. This command also resets the carriage position counter to zero thereby resetting the

control logic.

Slew to Selected Step Number and Stop. Upon command, the EUV carriage will slew to the step position which is contained in the control register at 50 steps per second and stop. While in this mode, changing the step position in the control register will automatically cause the carriage to slew to the new position and stop.

Scan about Selected Step Number. Upon command, the EUV carriage will scan about a selected step number at 6.25 steps per second. The range of the scan is 128 steps on either side of the selected step number unless limited by the end of travel at 12.0 or 64.0 nm. Scan will start in the long wavelength direction. Changing the step number in the control register will result in an automatic shift of the carriage to the new position and a continuation of the +128 step scan about the new position.

3.3.2 CIRCUIT DESCRIPTION - EUV CARRIAGE

The circuit provides inputs to the motor driver modules to execute the various maneuvers of the carriage mechanism. The modes of operation and a description of the circuit functions for each is described below. Drawing 47D231449 is referenced by zones in the description and is included as Figure 3.3-1.

Continuous Scan at 12.5 Steps per Second. Command labeled CD1 picks a latching relay (and resets all other command relays) to produce a HI state of the C1 signal ($\overline{C1}$ goes LO).

In Zone D-7, $\overline{C1}$ going LO produces a pulse to the direction flip-flop setting it to the LONG direction. In Zone B-11, C1 enables MPS 4 which comes from existing OSO-7 logic and is the 12.5 pps motor stepping signal. Assuming that

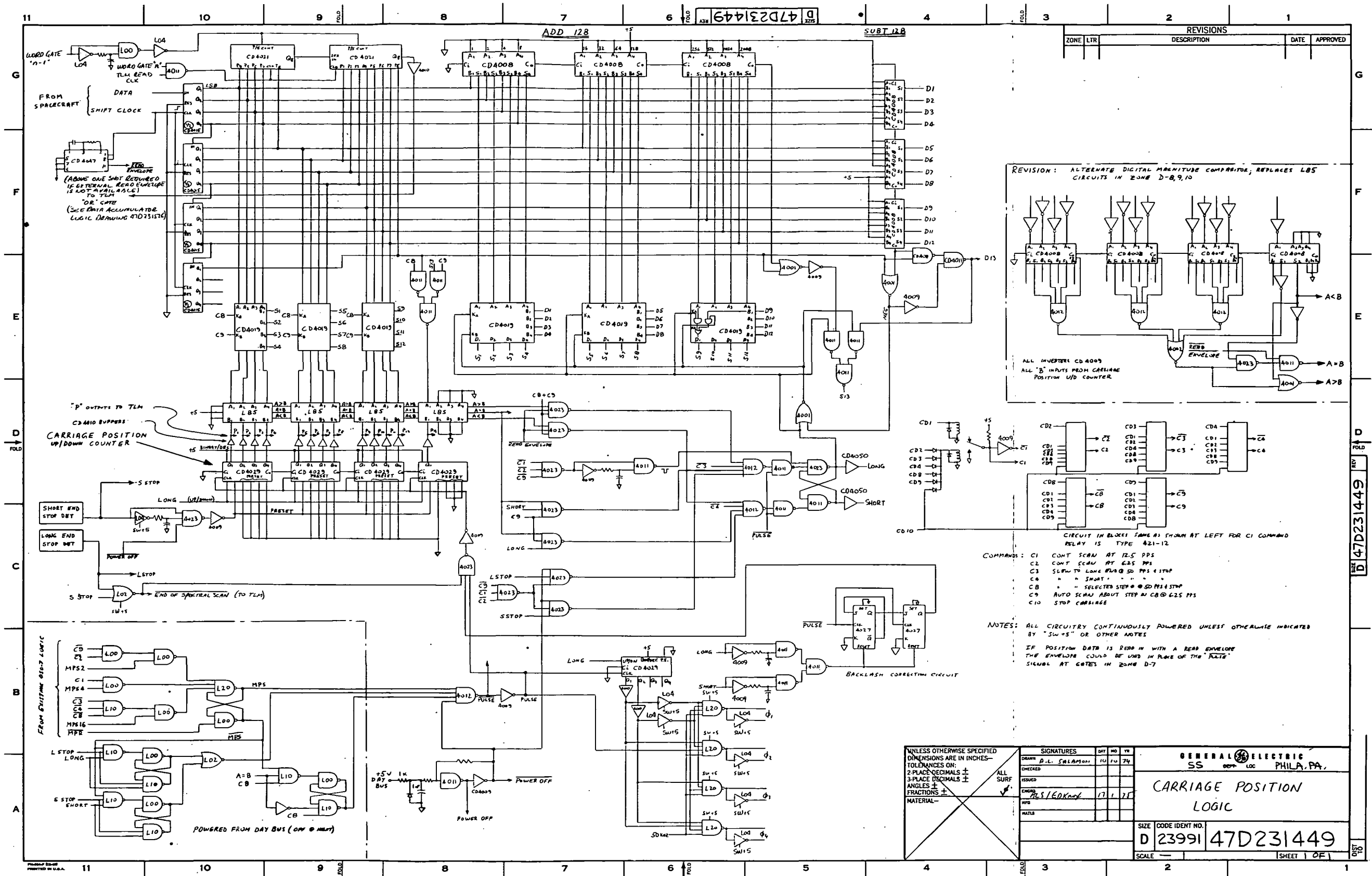


Figure 3.3-1. Carriage Position Logic

the carriage is not initially against the long end stop, the MPS signal pulsing at 12.5 pps passes through the gate at Zone B-8 and steps both the motor and the carriage position up/down counter (Zone D-10, -9, -8). Since the direction flip-flop is in the LONG state, the up/down counter will count up at each MPS pulse. The up/down counter (CD4029) in Zone B-6 controls the sequence in which the motor windings are energized. It is continuously powered and remembers *which winding was last energized---this being the count prior to each MPS pulse*. When the direction flip-flop is in the LONG state, the counter is commanded to count up and the count is decoded in such a sequence as to make the carriage move toward the long end. Thus the carriage moves toward the long end at 12.5 steps per second until the long end limit detector (Zone C-11) is tripped (L STOP = HI). In order to prevent foreshortening the motor pulse by sensing the stop before the motor pulse is finished, the $\overline{\text{PULSE}}$ signal is ANDed with the LSTOP and CI signals in gates at Zones C-7 and D-5. Thus when the motor pulse which drives the carriage into the stop is finished, a signal is produced which sets the direction flip-flop to the SHORT state. This causes both sets of up/down counters to be commanded to the count down mode so that at the next pulse, the sequence of motor pulses is reversed thereby causing the motor to drive toward the short end and the carriage position up/down counter to count down.

At the short end stop, the carriage position up/down counter is cleared to a count of zero; this periodically corrects the count and is the only true position feedback in this servo system (if no false counts occurred then the counter should already be at the proper count). When the carriage reaches the short end stop, the direction flip-flop is set to the LONG state by gates at Zones C-7 and D-5, and the process repeats as long as CI is HI.

Continuous Scan at 6.25 Steps/Sec. Command labeled CD2 picks a latching relay and resets all other command relays to produce a HI state on line C2 ($\overline{C2}$ is L0). The operation of this mode is exactly the same as for the one above except that the C2 signal selects "MPS2" which is the 6.25 pps pulse coming from existing OS0-7 logic (the selection occurs in gates in Zone B-11, -10).

Slew to Long End at 50 Steps/Sec and Stop. Command labeled CD3 picks a latching relay and resets all other command relays to produce a HI state of the C3 signal ($\overline{C3}$ is L0). $\overline{C3}$ sets the direction flip-flop to the LONG state and selects the MPS 16 which is the 50 pps pulse from existing OS0-7 logic. The carriage will slew to the long end until the stop is reached and L STOP signal goes HI. Signals L STOP, LONG (from direction flip-flop) and \overline{MPS} (to prevent foreshortening motor pulse) are ANDed in Zone S-11 and set a flip-flop to a state which inhibits all succeeding MPS pulses. The flip-flop stays in the inhibit state until the direction is set to the SHORT state and signal LONG goes L0. Since the direction flip-flop will not go to the SHORT state as long as the mode is selected, the carriage will remain against the LONG END stop.

Any other mode subsequently commanded will switch the direction flip-flop to the SHORT state. C4 does it directly (Zone C-6); C1, C2, C9 do it through gates in Zone C-8, -7; and C3 does it by producing an A<B signal in Zone D-8, -7.

Slew to Short End at 50 Steps/Sec and STOP. This mode operates exactly as the one above except roles of SHORT and LONG signals are interchanged. The MPS inhibit flip-flop is shown directly below the one discussed above (Zone A-10, -11).

Slew to Selected Step Number at 50 Steps/Sec. Command CD8 picks a latching relay and resets all other command relays producing a HI state for signal C8 ($\overline{C8}$ is LO). Prior to receiving command CD8, the desired step number should have been read into the serial in parallel out register (Zones E, F, G-10) from the spacecraft command system (See Section 3.13). The CD4019 select gates in Zones E-9, -10 route the number in the register to the digital comparators (Zone E, F-1, -2, -3) in response to the C8 signal at the K_A terminals being HI. The digital comparator compares this number to the number in the carriage position counter and produces a HI state on the appropriate output line; A>B, A<B, or A=B. For example, if the commanded step number is 3452, and the carriage is at step number 2470 at the time when CD8 is applied, then the A>B output will go HI since A = 3452 and B = 2470. A HI state on A>B when enabled by either C8 or C9 sets the direction flip-flop to the LONG state causing the motor to step toward the long end (long end is largest step number and short end is 0 step number). When the motor reaches the step number read into the register, the digital comparator will produce a HI on the A=B line (A>B will go LO) which, when ANDed with the C8 and \overline{MPS} signal in Zone A-10, sets a flip-flop to a state which inhibits further pulses to the motor (and counter). Again, the \overline{MPS} signal is utilized to prevent cutting the motor pulse short. The inhibit flip-flop is not reset until the system is taken out of the CD8 mode or until A=B goes LO in response to a new number read into the position command register, and therefore, the carriage will remain at the selected step number. If the carriage is at a larger step number than that which is commanded, the comparator will produce a HI on the A<B line and the direction flip-flop is set to the SHORT state causing the carriage to move toward the short end until it reaches the desired step number.

Scan about Selected Step Number at 6.25 Steps per Second. Command C9 picks a latching relay and resets all other command relays causing C9 to go HI. Since C8 has been superceded, the inhibit flip-flop mentioned in the above paragraph is reset allowing MPS pulses at 6.25 pps to propagate through the inhibit gate at Zone B-8. C9 does not destroy the information read in the control register which corresponds to the desired step number of the C8 mode. This step number is used as one set of inputs to each of two full adder circuits composed of CD4008 devices and shown in Zones G-6, -7, -8 and G, F-4. One set of full adders adds a hard wired count of 128 to the number in the register producing an upper limit of $n + 128$. The other adder has a hard wired 2's complement of 128 and thus subtracts 128 from the number in the register producing a lower limit of $n-128$. The direction flip-flop is initially set to the LONG state by C9 through gate and differentiator at Zone D-7, and this causes the CD4019 select gates at Zone E-6, -7, -8 to connect the adder outputs ($n + 128$) to the S₁ through S₁₃ lines; these lines in turn are routed to the digital comparitors (Zone E, F-1, -2, -3) through select gates (Zone E-9, -10) by the C9 signal being HI at the K_B inputs. Thus the initial comparison is between the present carriage position count and the $n+128$ number. Since typically mode C9 will follow C8, the carriage will initially be at count n and therefore, $A>B$ will go HI causing the motor pulse toward the long direction. When the carriage reaches step number $n+128$, signal $A=B$ will go HI, and gates in Zone C-7 will produce a signal to set the direction flip-flop to the SHORT state. This causes the LONG signal to go LO and through the NOR gate at Zone D-5, the K_B inputs to the selected gates will be energized causing the $n-128$ number to be routed to the digital comparitor. Since $n-128$ is less than $n+128$ (the last previous step), the comparitor produces a HI on the $A<B$ line; the motor will step toward the SHORT end until it reaches step number $n-128$. The gates

at Zone C-7 route the $A=B$ to set the flip-flop to the LONG state again. This process is repeated as long as C9 is HI.

If $n-128$ is a negative number, which would indicate a position beyond the short end stop, the NOR gate in Zone E-4 will produce a HI output which will force the signal to K_B of the select gates to go LO and since the signal at K_A is already LO, S_1 through S_{13} will read 0. Thus, the lower limit will be 0 instead of a negative number.

If $n+128$ happens to be a larger number than the number corresponding to the LONG end STOP, then the carriage will drive into the LONG end stop and signal L STOP through gate at Zone C-7, will set the direction flip-flop to the SHORT state, and the carriage will reverse direction at the next motor pulse. Thus in mode C9, the carriage will scan ± 128 steps to both sides of the number read into the register unless a stop is reached first in which case it will merely turn around, the other turn-around point is not affected by the stop.

A change to ± 64 steps may be accomplished by changing the hardwired inputs to the adder and subtractor---changing two wires from ground to +5, and two wires from +5 to ground.

The central position of the auto scan can be changed at any time during a scan without additional CD8 or CD9 commands by merely reading in a new number into the register.

Stop Carriage Command. Command CD10 resets all command relays and in the absence of any of the commands (C1, C2, C3, C4, C8, C9), no MPS pulses are gated through and the motor will not step.

Additional Features. The circuitry in Zones A-10 and -11 provide a backup to

prevent a motor from driving into the stops in case the normal circuit functions fail. The combination of L STOP and LONG signals or S STOP and SHORT signals will set flip-flops to the inhibit state preventing further motor pulses until the direction flip-flop changes state.

A $\overline{\text{POWER OFF}}$ signal is generated in Zone A-8 when the day bus power is removed. This signal inhibits the MPS pulses and since all critical circuitry remains powered and no pulses are getting in, the circuit will hold the last state at the time power was turned off. The $\overline{\text{POWER OFF}}$ signal is such that it goes LO (inhibit state) with no delay when power goes off, but it goes HI (enable normal operation) with a 1 ms delay giving time for the switched circuitry to settle down before the carriage position logic is enabled.

The commands from the spacecraft are assumed to be as for OSO-7, i.e., pulses with sufficient drive capability to switch ten 500 ohm latching relays in parallel. The command priority is such that all new commands supersede and destroy the memory of previous commands.

The logic drawing indicates all circuitry which has switched power; all unmarked circuits are continuously powered.

The circuit interfaces directly with present OSO-7 logic requiring MPS 2, MPS 4, MPS 16, $\overline{\text{MPR}}$, as inputs and providing \emptyset_1 , \emptyset_2 , \emptyset_3 , \emptyset_4 as outputs to the motor driver modules. The interface with the spacecraft consists of seven mode commands (pulses to set latching relays), two lines to load the step number (shift line and number line).

The circuitry in Zones B, C-4, -5, -6 was added to compensate for backlash in the gears driving the carriage. The two differentiators in Zone B-5 produce

a pulse whenever the direction flip-flop changes state. This pulse resets the two CD4027 J-K flip-flops so that the Q output goes LO and inhibits pulses to the carriage position counter for two pulses. The trailing edge of the second pulse clocks the second flip-flop so that Q goes HI and subsequent pulses will be counted. In effect, this circuit allows two motor pulses which are not counted at each change of direction; the backlash on OSO-7 was equivalent to two motor pulses. Backlash correction also occurs at the stops where the pulses to the counter are inhibited as long as the stop detectors are tripped; this is done by using the output of the L02 gate in Zone C-11 to inhibit pulses at the CD4023 gate of Zone C-8.

The outputs of the digital comparator must be inhibited while a new number is being read into the register of Zone E, F, G-10 so that temporary false outputs of the comparator do not change the state of the direction flip-flop (and thus trigger the backlash correction circuit resulting in a 2 count error in position). This can be accomplished by using the read envelope signal to inhibit the comparator outputs in the gates in Zone D-7. The read envelope signal may be available from the spacecraft, but if it is not, then it can be generated by the monostable multivibrator, CD4046, shown in Zone F-11.

3.4 CONTROL OF EUV EXIT APERTURE MASK

This portion of the study was directed toward improving the operational capability of the mask which selects the appropriate set of exit apertures on the EUV carriage. The study was to develop the capability to command the mask to position A (longer wavelength apertures) or position B (shorter wavelength apertures) without knowledge of the actual position. The ability to automatically change the position of the mask at the end of each large raster will be maintained. The requirement to automatically change the position of the mask

only at the end of two consecutive large rasters was deleted.

3.4.1 MODES OF OPERATION

The EUV Exit Aperture Mask has three modes of operation. These modes of operation are described below.

Select Mask Position A. Upon command, the mask will move to position A which will illuminate the longer wavelength set of apertures. No movement will occur if the mask is in position A.

Select Mask Position B. Upon command, the mask will move to position B which will illuminate the shorter wavelength set of apertures. No movement will occur if the mask is in position B.

Switch Mask Position at EOR. Upon command, the mask will change position upon receipt of the end of raster (EOR) pulse. This mode of operation will continue until either the Select Mask Position A or Select Mask Position B command is given.

3.4.2 CIRCUIT DESCRIPTION - EUV EXIT APERTURE MASK CONTROL

The changes to the EUV mask position logic are relatively minor (refer to Drawing 47C217126, sheet 10, for the OS0-7 configuration and Drawing 47C231447 for the revised version). Drawing 47C231447 is referenced by zones in the description and is included as 3.4-1.

Select Mask Position A or B. The direction flip-flop had to be changed to accommodate one additional input to each side (set and reset sides). One of these new inputs is the $\overline{CT3}$ (Select Mask Position A NOT) signal to the same side as the "MS4" input; either of these signals going LO will reset the flip-flop so that the counter counts down and causes motor pulses in a sequence to

cause movement toward mask Position A. The other new input is $\overline{C14}$ (Select Mask Position B NOT) to the same side as the "MS3" input; either of these signals going LO will cause the counter to count up and the motor will move toward Mask Position B. Also, the 2 wide "AND-OR-INVERT GATE" (OS0-7) had to be changed to a 4 wide AND-OR-INVERT GATE to accommodate the C13 and C14 inputs (see Zone B, C-7). This change allows setting the enable flip-flop (Zone B-6) to the enabled state whenever the "Select Mask Position A" command (C13) is received and the mask is not already at position A (MS3 is HI) or when the "Select Mask Position B" command (C14) is received and the mask is not already at position B (MS4 is HI).

Change Position at End of Raster (EOR). In Zone C-7, the signal "SORP" is ANDed with C15, the "Auto Switch at End of Raster" signal to produce a clock pulse to the flip-flop in Zone B-6 and to initiate a change in mask position. This mode is unchanged from the OS0-7 design.

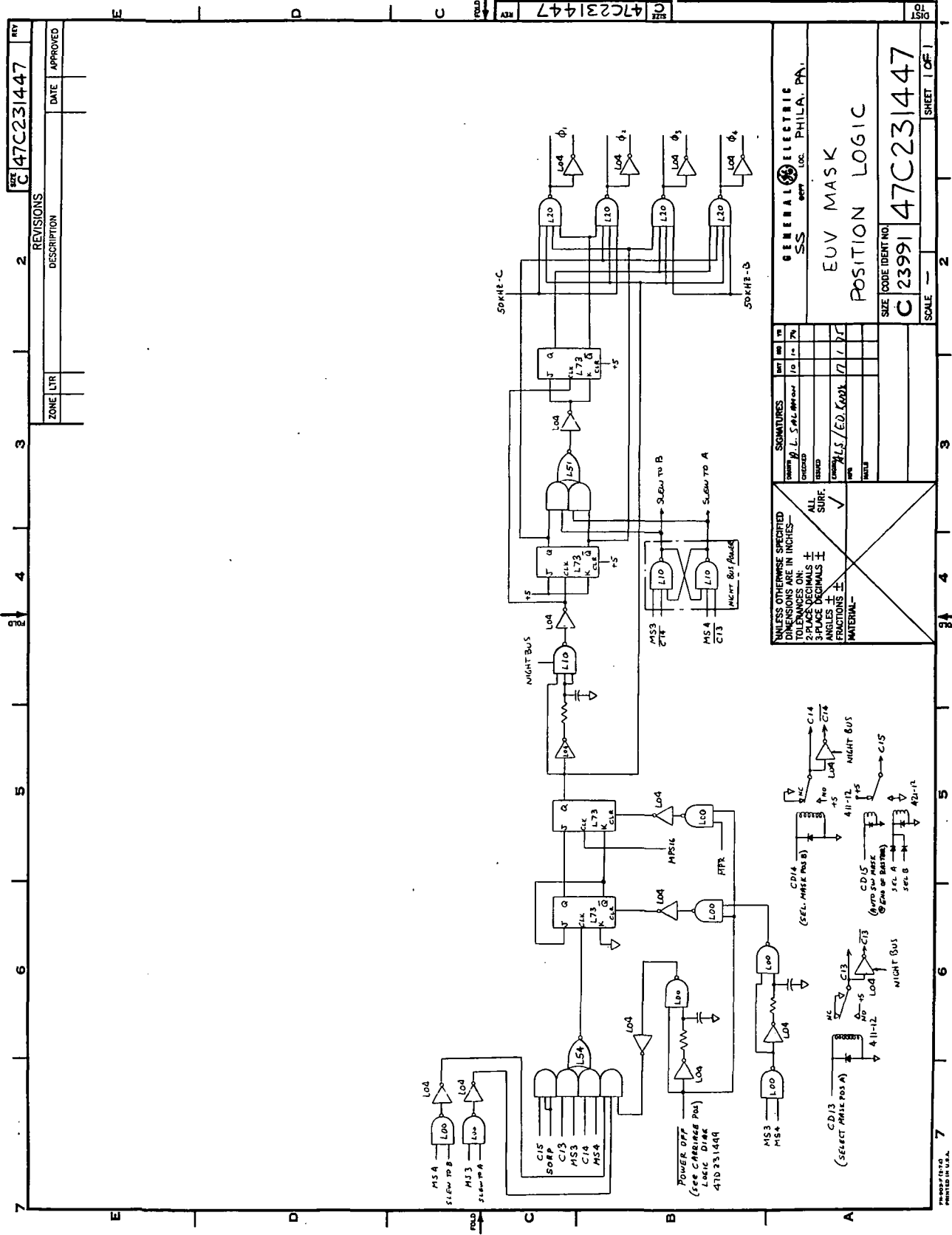
Additional Features. The circuits within the outlined areas of Figure 3.4-1 are powered continuously from the night bus.

The following changes to the OS0-7 logic were also made:

(a) Combined the \overline{MRP} and $\overline{POWER OFF}$ signals in an OR gate in Zone B-5 to prevent a false motor pulse at power turn on. The $\overline{POWER OFF}$ signal at that point is generated as shown on the new logic drawing for the EUV carriage position logic.

(b) Added 2 input gate and inverter to Zone B-6 to allow a forced "clear" of the enable flip-flop by the $\overline{POWER OFF}$ signal.

(c) Added a circuit in Zone B-6, -7 to differentiate the $\overline{POWER OFF}$ signal and



REV	DATE	APPROVED
2		

ZONE	LT/R

REV	DATE	APPROVED
2		

ZONE	LT/R

REV	DATE	APPROVED
2		

REV	DATE	APPROVED
2		

Figure 3.4-1. EUV Mask Position Logic

to allow this differentiated pulse to set the enable flip-flop to the enabled state when MS3 and MS4 are both HI. The purpose of this item is as follows: If day bus power is turned off while the mask is changing positions, then upon return of Day Bus power, the enable flip-flop needs to be set so that the motor resumes its motion and completes the command it was executing. The $\overline{\text{POWER OFF}}$ signal stays LO about 1 ms after day bus goes ON thus per item (b) above, the enable flip-flop is reset. However, we want this flip-flop in the set state under these conditions so that the $\overline{\text{POWER OFF}}$ signal is differentiated and a HI going pulse is produced at the trailing edge. Thus if the mask is between stops (MS3 and MS4 both HI), the flip-flop receives a clock pulse after the clear goes HI and the flip-flop will be clocked to the enable state. Then after one of the stops is reached, reset occurs through differentiator (Zone A-6, -7).

Since the changes to this portion of the logic are minor, we have retained the 54L series logic for the continuously powered gates which will contribute 3 mw of power to the night bus requirements. The 3 mw value could be reduced to less than 1 mw by changing the continuously powered gates to CMOS devices.

It should be noted that the L73 flip-flops comprising the counter in Zone B, C-3, -4 do not require continuous power since losing count during the power-off period merely means that the motor may not step properly for the first 2 pulses. However, since position indication is not dependent on counting motor pulses, this will not present a problem.

3.5 CONTROL OF X-RAY FILTER WHEELS

This portion of the study was directed toward the definition of the changes required to command either filter wheel directly to any of the six filter

wheel positions without first stopping the filter wheel to permit position update. The balance of the OSO-7 operational requirements were to be retained.

3.5.1 MODES OF OPERATION

Each of the X-Ray filter wheels have three modes of operation which are defined below.

Advance Every 5.12 Seconds. Upon command, the filter wheel will automatically advance one filter position at the end of each 5.12 second interval. The filter wheel will continue to advance until one of the other modes is selected by command.

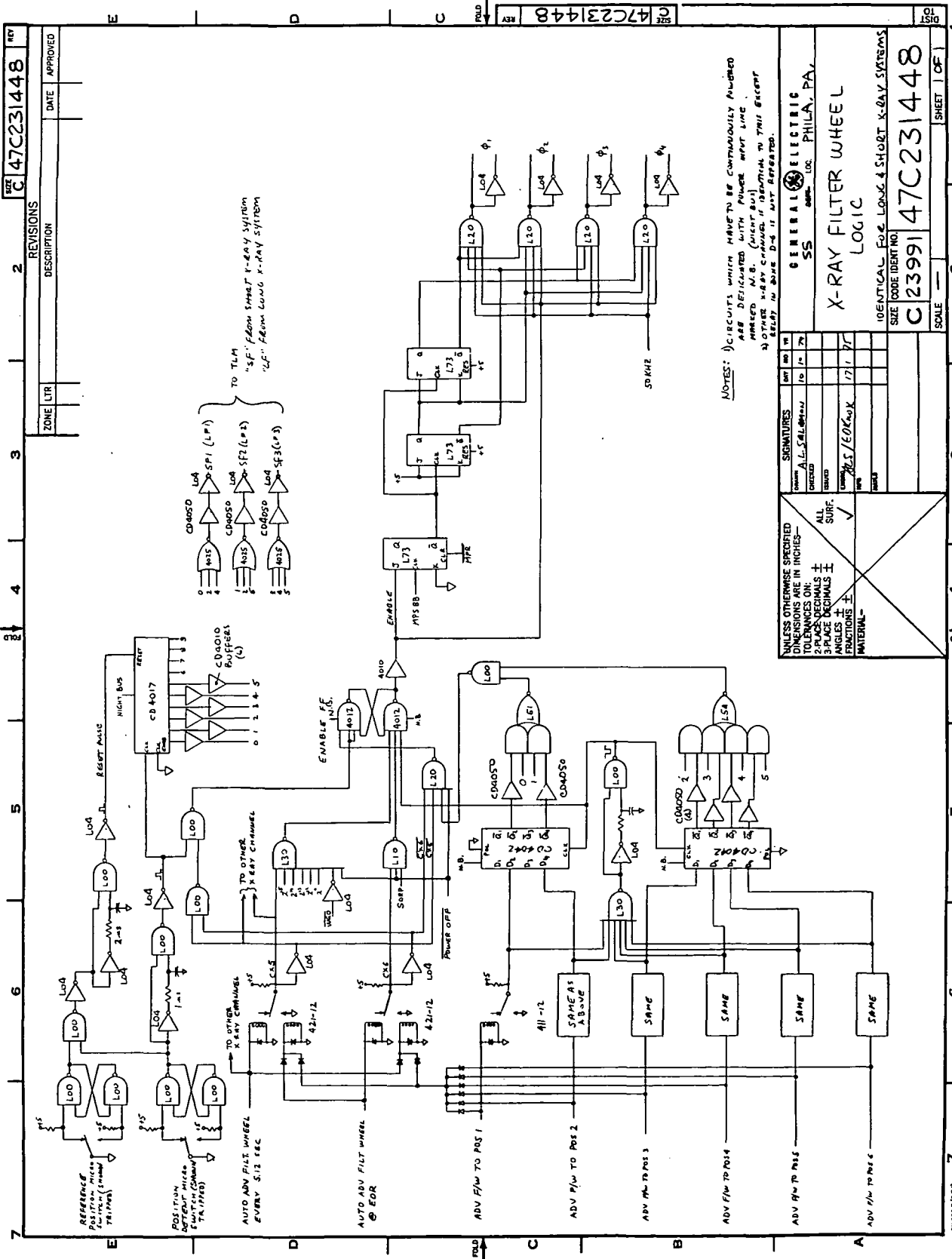
Advance at EOR. Upon command, the filter wheel will advance one filter position at the end of each large raster. The filter wheel continues to advance until one of the other modes is selected by command.

Advance Filter Wheel to Selected Filter. Upon command, the filter wheel will advance to the filter position selected (one of six positions) and stop. The filter wheel will not move if commanded to go to its current position.

3.5.2 CIRCUIT DESCRIPTION - X-RAY FILTER WHEEL CONTROL

The filter wheel rotates in one direction only when commanded. A microswitch detects the rotation by means of detents located at each filter position. A second detent is provided at filter position number one and is detected by a second microswitch for use as a reference position. The operation of the circuits are described below. Drawing 47C231448 is referenced by zones in the description and is included as Figure 3.5-1.

Advance Every 5.12 Seconds. This mode is initiated by a command pulse which sets the relay in Zone D-6 and resets the relay in Zone C-6. The setting of



NOTES: 1) CIRCUITS WHICH HAVE TO BE CONTINUOUSLY MONITORED ARE DESIGNATED WITH POWER WIRE LINE MARKED N.B. (NIGHT BUS) 2) OTHER X-RAY CHANNELS IDENTICAL TO THIS EXCEPT RELAY IN SHIRT D-6 IS NOT REPEATED.

SIGNATURES		DATE	BY
DESIGNED	A. S. L. / M. J. / J. W.	10	79
CHECKED			
DESIGNED	M. S. / E. O. / K. W.	17	77
CHECKED			
UNLESS OTHERWISE SPECIFIED DIMENSIONS ARE IN INCHES— FRACTIONS ONLY ± 3-PLACE DECIMALS ± ANGLES ± FRACTIONS ± MATERIAL			
GENERAL ELECTRIC PHILA., PA. X-RAY FILTER WHEEL LOGIC IDENTICAL FOR LONG & SHORT X-RAY SYSTEMS SIZE (CODE IDENT NO.) C2399147C231448 SCALE 1:1 SHEET 1 OF 1			

Figure 3.5-1. X-Ray Filter Wheel Logic

the first relay causes line "C X 5" to go HI thus enabling the gate in Zone D-5 to decode the proper word gate (WG) and sub frame word (SFW) combination which occurs every 5.12 seconds and is used to time the interval between filter wheel advances. The 2^{11} to 2^{15} inputs come from the "Timing Generation Logic" Drawing (see Figure 3.7-1) and represent outputs of the basic counting chain.

Decoding the proper signals in the above gate produces a LO at the output which sets the enable flip-flop to the enabled state. This in turn enables the motor phase/pulse decoders in Zone B, C-2 and the L73 flip-flop in Zone C-4 to produce clock pulses to the counter (Zone C-3). Thus \emptyset_1 through \emptyset_4 are decoded in sequence and the motor will step at 25 steps/sec (the rate of the MPS 8B input to the L73 flip-flop). When the wheel reaches the next position, the microswitch is tripped by the detent and the differentiator in Zone E-6 produces a pulse which is gated through an L00 gate (Zone E-5) to reset the enable flip-flop; thus stopping further motor pulses. The above L00 gate is enabled by either of the two automatic advance commands having been selected (C X 5 or C X 6 HI). The motor remains stopped until the proper combination of word gate and sub frame is decoded again (nominally 5.12 seconds later), and the above sequence is repeated until stopped by the next position detent.

Advance at End of Raster. This mode is initiated by a command pulse which sets the relay in Zone C-6 and resets the relay in Zone D-6. The setting of the first relay produces a HI on line "C X 6" which then enables the "SORP" pulse (Start of Raster Pulse) to pass through the L00 gate in Zone C-5 to the set side of the enable flip-flop. From this point on, the operation is exactly as described above for the other automatic advance mode; the only difference in the two modes is that in this mode, motion is initiated by the "SORP"

signal (from present OSO-7 logic) whereas in the other mode, it is initiated by decoding the proper word gate and sub frame signals.

Advance Filter Wheel to Selected Filter Position. This mode is initiated by one of six command pulses corresponding to the six positions which can be selected. Any of the six command pulses will reset the command relays of the two automatic advance modes; thereby superceding those modes. The six commands each go to the coil of a normal relay to provide isolation between the command system and the experiment (same as in OSO-7). Energizing any of these relays will produce a LO (ground) on the logic line connected to the wiper of the relay (normally open contact is grounded). These six logic lines each go to a "D type Latch" (CD4042) and to a six input OR gate which drives a differentiator. Thus the differentiator will produce a pulse when any of the six relays is energized. This pulse is connected to the clock input of the above CD4042 latches and causes these circuits to remember which relay had been energized---the CD4042 circuits are powered from the night bus and, therefore, provide nonvolatile storage of the last commanded position. Since the relay wiper returns to its normal state after the command pulse stops, the CD4042 latches are the only means of remembering the last command; any subsequent clock pulse to these circuits will destroy the information stored and read in whatever is on the inputs at that time; thus, new positions can be commanded with the latest taking priority over all previous ones. The above differentiator also sets the enable flip-flop so that the motor is enabled to pulse until the commanded position is reached. This is accomplished as follows:

A CD4017 counter counts the pulses which are produced each time the microswitch detects a detent at each of the six filter positions (pulses are shaped by the bottom differentiator in Zone E-6). A second microswitch detects a detent

only at the reference position (position 1) and produces a pulse (top differentiator in Zone #-6) which resets the counter to a count of 0. In order to prevent a race condition between the two microswitches, the signal from the reference microswitch is ANDed with the signal from the normal position microswitch before it goes into the differentiator. Thus, the reset pulse cannot occur ahead of the clock pulse and it is assured that the reset occurs last and that the counter will be at 0 after position 1 is passed. The CD4017 counter has internal decoding and outputs "0" through "9" go HI in sequence at each clock pulse; thus the only output which is HI is the one corresponding to the position last reached. The "0" through "5" outputs of this counter are compared to the information stored in the CD4042 latches by a 54L51 and a 54L54 AND-OR-INVERT gate. When the counter reaches the count corresponding to the commanded position, one of these gates will produce a LO resulting in a HI at the output of the L00 gate in Zone C-4. This HI is ANDed with the $\overline{CX5}$ and $\overline{CX6}$ signals to produce a reset pulse to the enable flip-flop which will stop the motor pulses. The ANDing of the $\overline{CX5}$ and $\overline{CX6}$ signals insures that the enable flip-flop can only be reset in this manner when neither of the Auto Advance modes is selected which in turn implies that the "Advance to Selected Position" mode is selected. The counter will keep track of the position of the filter wheel regardless of the mode (and hence can be used to originate TLM information), but only in the "Advance to Selected Position" mode can it stop the motor when the selected position is reached.

The flip-flops in Zone C-2, -3, -4 do not need continuous power since position indication is not dependent on counting motor pulses. If, after power shutdown, these flip-flops come up in a state such that the next motor pulse causes a backward step of the motor (or no step at all), this will not cause a

problem since the sequence of \emptyset_1 through \emptyset_4 will be correct, even though the initial phase selected may be wrong; and, eventually, the phases will catch up to the motor position and proper operation will commence. (Worst cases are one backward step or two pulses with no steps before normal operation resumes.)

3.6 DATA PROCESSING

This portion of the study was directed toward the increase in data output of the instrument. The basic requirement was to provide simultaneous readout of the three EUV channels, the H-Alpha channel and the four X-Ray channels. The capability to readout Channel A, Channel B, or Channel A-B on one data channel was to be retained for the long and short X-Ray systems. Data compression was to be provided for all data channels.

The logic diagram of this circuitry (Drawing 47D231526) shows data accumulators (counters) for the SHORT EUV, LONG EUV, SHORT X-RAY A ONLY and SHORT X-RAY A, B or (A-B) channels. It also shows the data compression logic servicing these four data channels. The medium EUV and Long X-RAY A ONLY and LONG X-RAY A, B or (A-B) channels and their data compression logic are not shown on the drawing. However, they are identical to the logic shown with the exception that the word gates used to stop and start accumulation and compression as well as those used to enable data readout will be different. Drawing 47D231526 is referenced by zones in the following discussion and is included as Figure 3.6-1.

The logic is basically the same as for OSO-7 with the following exceptions:

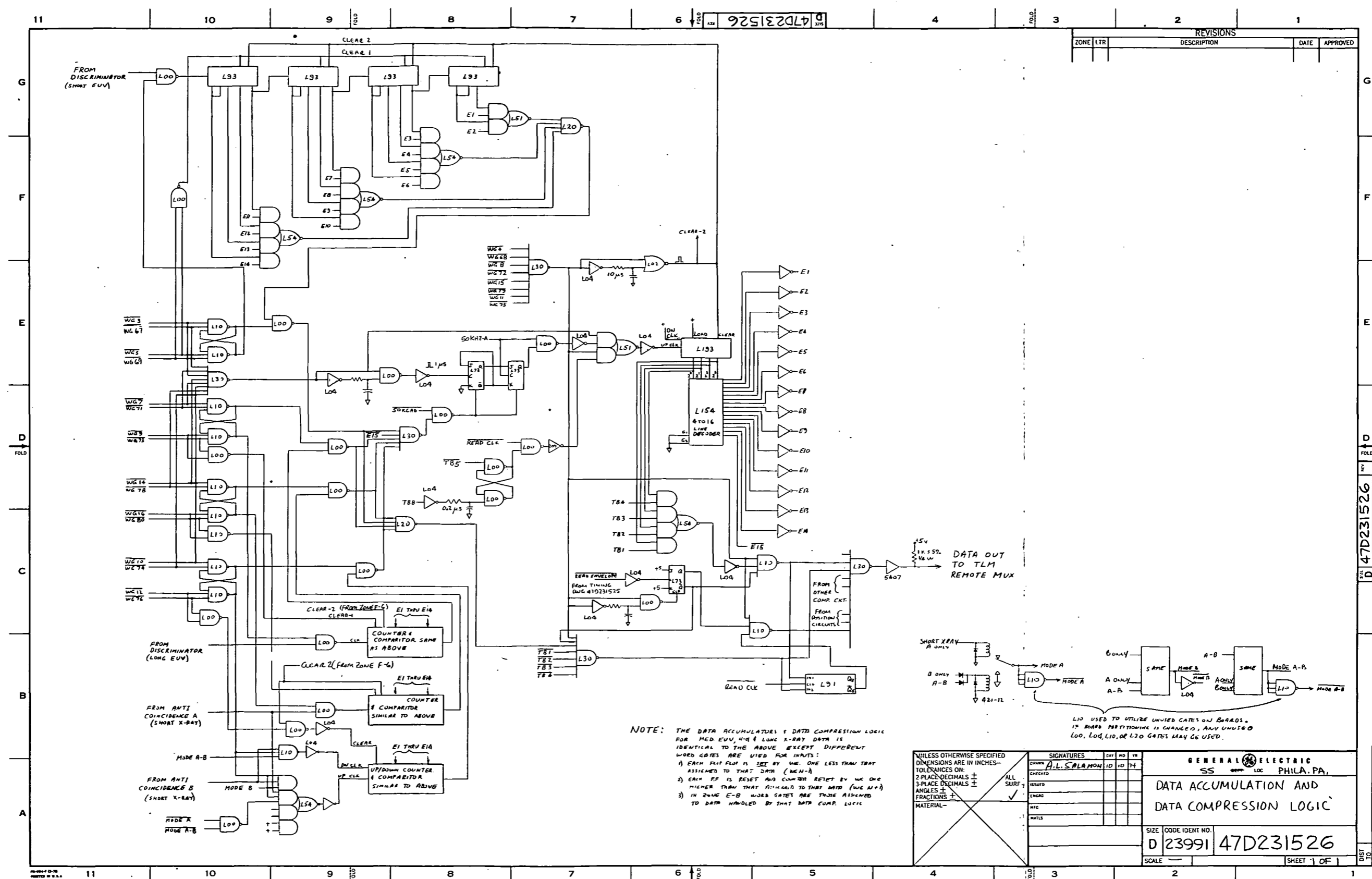
- 1) Bit times are not used to decode start and stop times; instead, word gates only are used.

- 2) Data accumulation time has been changed to 77.5 ms with 2.5 ms allotted for data compression and readout giving an 80 ms period as compared to 160 ms for OSO-7.
- 3) Some MSI circuits (L93, L193 and L154) are used to reduce package count to about half of what it was for OSO-7.
- 4) Logic is added to allow reading the same data twice per word period since this can be required where OSO-I type TLM formatters are used (study program requirement, see Section 3.7).

Since the data compression counter is used in the data readout process, adjacent words cannot be handled by the same data compression circuit. If adjacent data words are assigned, then the two compression circuits must be interleaved to handle alternate data words.

The operation of the circuitry is described for the SHORT EUV channel; the others are identical except for word gates used: The SHORT EUV data is assigned to TLM words 4 and 69 of each minor frame making them 80 ms apart (the assignments are assumed for illustrative purposes---other word combinations could be used provided the two words in the minor frame are separated by 64; See Section 3.7).

As a starting point, assume that the counter (four L93 stages) in Zone G-8, -9, -10 is counting, i.e. the enable input to the L00 gate in Zone G-10 is HI. At the start of TLM word time number 3, the signal $\overline{WG3}$ goes LO and sets the flip-flop in Zone E-10. This causes the enable input to the L00 gate to go LO and pulses from the discriminator are inhibited from going into the counter (counting stops, but number in counter is not destroyed). $\overline{WG3}$ also goes to the L30



ZONE		LTR		DESCRIPTION	DATE	APPROVED

NOTE: THE DATA ACCUMULATION & DATA COMPRESSION LOGIC FOR MED EUV, HRA & LONG X-RAY DATA IS IDENTICAL TO THE ABOVE EXCEPT DIFFERENT WORD GATES ARE USED FOR INPUTS:
 1) EACH PULF FLOW IS SET BY ONE LESS THAN THAT ASSIGNED TO THAT DATA (NEN-1)
 2) EACH FF IS RESET AND COUNTER RESET BY ONE HIGHER THAN THAT ASSIGNED TO THAT DATA (WEN+1)
 3) IN ZONE E-B WORD GATES ARE THOSE ASSIGNED TO DATA HANDLED BY THAT DATA COMP. LOGIC

SIGNATURES		DATE	NO.	BY
DRAWN	AL SALAMON	10	10	74
CHECKED				
DESIGNED				
ENG'G				
MFG				
MAINT.				

GENERAL ELECTRIC		PHILA. PA.	
DATA ACCUMULATION AND DATA COMPRESSION LOGIC			
SIZE	CODE IDENT NO.	47D231526	
SCALE	SHEET 1 OF 1		

Figure 3.6-1. Data Accumulation and Compression Logic

gate in Zone E-10 which is performing an OR function, its output going HI when any input goes LO. Thus through the L30 gate when $\overline{WG3}$ goes LO, the differentiator in Zone E-9 produces a pulse which clocks the first L73 flip-flop so that its Q output goes HI. Since Q is connected to the J input of the next flip-flop, the very next falling edge of the 50 KHz clock causes the Q output of the second flip-flop to go HI enabling the L00 gate so that the succeeding pulses of the 50 KHz can pass through this gate and into the L193 counter in Zone E-6. The purpose of these two L73 flip-flops is to synchronize the gating through of the 50 KHz so that no partial pulses, or slivers, get through.

The L193 counter now starts to count pulses at the 50 KHz rate, and the L154 decoder produces HI outputs successively and one at a time from E1 through E14 (Zone C, D, E-5). These outputs successively enable the L51 and L54 gates in Zone F, G-8, -9, -10 and effectively address each bit of the counter starting with the right most or MSB bit. When the first HI state (or 1) is found in this manner, the output of the L20 gate in Zone F-7 goes HI and is gated through the L00 gate in Zone E-9 and through the OR gate (L30) in Zone D-8, and resets the two L73 flip-flops on the next LO state of the 50 KHz clock. This inhibits further pulses of the 50 KHz from getting to the counter, and the count appearing at the 2^0 to 2^3 outputs of the counter (Zone E-6) is the binary equivalent to the position of the first "1" in the short EUV accumulator. This completes the data compression function which all took place during word 3.

During word 4, the L30 gate at Zone E-7 produces a HI output which enables the L10 gate in Zone C-5 and the 2^3 to 2^0 outputs of the compression counter are routed to the TLM output one at a time during bit times TB1 through TB4. TB1 through TB8 are generated on the Timing Generation Logic Drawing (see Figure

3.7-1) and are HI during data bit times 1 through 8 respectively. At the start of bit time 5, the $\overline{TB5}$ signal sets the flip-flop in Zone D-8 to the enable state so that the $\overline{READ\ CLOCK}$ signal is enabled and is routed to the compression counter (L193 in Zone E-6) which steps and addresses the next bit of the accumulator. The state of this next bit is routed through the L20 gate in Zone F-7, through the L00 gate in Zone E-9, through L20 gate in Zone C-8, and through the L30 gates in Zones B-7 and C-5 to the TLM output. On each succeeding transition of the READ CLOCK, the compression counter is advanced and the next bit of the accumulator is addressed and routed to the TLM output. The same 8 bits which go to TLM are also read into the L91 shift register in Zone B-5. At the end of the 8th bit, the $\overline{READ\ ENVELOPE}$ signal goes HI and the L73 flip-flop is clocked so that the \overline{Q} output goes LO, this inhibits data from passing through the L10 gate in Zone C-5 and the L30 gate in Zone B-7 and since Q has gone HI, it enables data from the L91 shift register to go to TLM. Thus, when both OSO-I type TLM formatters are operating, the data can be read out a second time from the shift register by the second group of READ CLOCK pulses.

At the beginning of word time 5, $\overline{WG5}$ going LO resets the flip-flop in Zone E-10, this enables the accumulator to count discriminator pulses again. However, before this happens, the differentiator in Zone E-6, -7 produces a 10 μ s wide pulse when WG4 ends and this is ANDed in the L93 counters with the WG5 or WG69 signal to reset the accumulator.

This process is repeated in the short EUV channel starting with WG67 and ending with WG69 to produce the second data word of each minor frame (80 ms apart). The process is also identical for the other data channels.

None of this circuitry requires Night Bus Power since a power shutdown only causes loss of one 80 ms period of data.

3.7 TIMING AND TELEMETRY CIRCUITRY

The TLM data rate and format will be different from the OSO-7 configuration; therefore, significant changes to the existing design will be required.

The revised design is based upon OSO-I Telemetry specifications (SS 31331-400, Rev. D, pages 94 through 123, and SS 31331-006, Rev. B, pages 5, 6, and 7)*supplied by NASA/GSFC. With the above specifications, certain assumptions had to be made since the allocation of telemetry words will not be made during this study phase. Based upon NASA/GSFC requirements that the data sampling rate should be more frequent than for OSO-7, we have assumed that science data for each channel will be sampled twice per minor frame at 80 ms intervals. The 80 ms interval puts a restriction on the word assignments such that each pair is 64 words apart. (Each minor frame has 128 words, and the time per minor frame is 160 ms.) Since certain words in the minor frame are dedicated to certain spacecraft functions, the following words could possibly be available: Number 4 through 25, 28, 31, 36 through 57, 68 through 76, 78 through 95, 100, 103 through 111, 113 through 126. With 80 ms between pairs, the following pairs would be usable:

4-68	12-76	21-85	39-103	47-111	56-120
5-69	14-78	22-86	40-104	49-113	57-121
6-70	15-79	23-87	41-105	50-114	
7-71	16-80	24-88	42-106	51-115	
8-72	17-91	25-89	43-107	52-116	
9-73	18-82	28-92	44-108	53-117	
10-74	19-83	31-95	45-109	54-118	
11-75	20-84	36-100	46-110	55-119	

*Hughes Aircraft Co. Specifications

A further uncertainty is the assignments of TLM channels to the X-Ray data. If each X-Ray channel has only one data word (select A, B or A-B), then a total of 6 lines of data have to be accommodated; however, if the X-Ray channels have an A only output, then 8 lines of data result. For purposes of this design, we have assumed the worst case of 8 lines of data each sampled twice per minor frame resulting in 16 words and an additional 8 words for position information for a total of 24 words (out of 128) per minor frame dedicated to the instrument.

Another area of uncertainty is how these 12 lines of data will be sent to the TLM system. The multiplexing could be done inside the instrument resulting in only one line of data in the experiment to Remote MUX interface. Alternately, the 12 items of data could be sent on 12 wires to the remote MUX; this would also require 12 lines for the read envelope signals.

For the study design, we have arbitrarily assumed the following word assignments:

<u>Word Number</u>	<u>Data</u>
4, 68	Short EUV
5, 69	Medium EUV
6, 7, 70, 71	Carriage Position
8, 72	Long EUV
9, 73	Aperture Position
10, 74	H- α
11, 75	Short X-Ray, A, B, or A-B
12, 76	Filter Wheel Positions (Short and Long)
14, 78	Long X-Ray, A, B or A-B
15, 79	Short X-Ray A only
16, 80	Long X-Ray A only

and the multiplexing was done in the instrument. Thus the interface between

the spectroheliograph and the remote multiplexer will consist of one line for the READ ENVELOPE, one line for the TLM READ CLOCK, and one line for DATA. We also require the "6.4 KHz BIT CLOCK" and the "TLM Major Frame Rate" (20.48 sec period) signals to synchronize our multiplexing to the telemetry frame. In addition to the 8 science data words, we require 4 words to transmit the carriage position, aperture wheel position, and the position of the two filter wheels. These words have to be transmitted at the same rate as the data so that the position at which the data was taken is known. Since there are 13 bits of carriage position data, two TLM words are required for this information leaving 3 bits unused which could be assigned to other housekeeping data and even subcommutated within the experiment to handle a large number of binary data items such as mask position, microswitch closures, state of command relays, etc. (It would be of little use for analog monitors such as thermistors since only 3 bits are available, and the resulting resolution would be poor.) There are two bits left over from the filter wheel position word since each filter wheel requires 3 bits to encode its position.

The 6.4 KHz bit clock is also used to count down and generate the motor pulses for the various stepping speeds. The rate and duty cycle for each stepping rate is identical to the OSO-7 instrument. The pulses are decoded such that no leading edge occurs during the word when the position information is loaded into the TLM output register insuring that position information is never read when the position up/down counters are changing state.

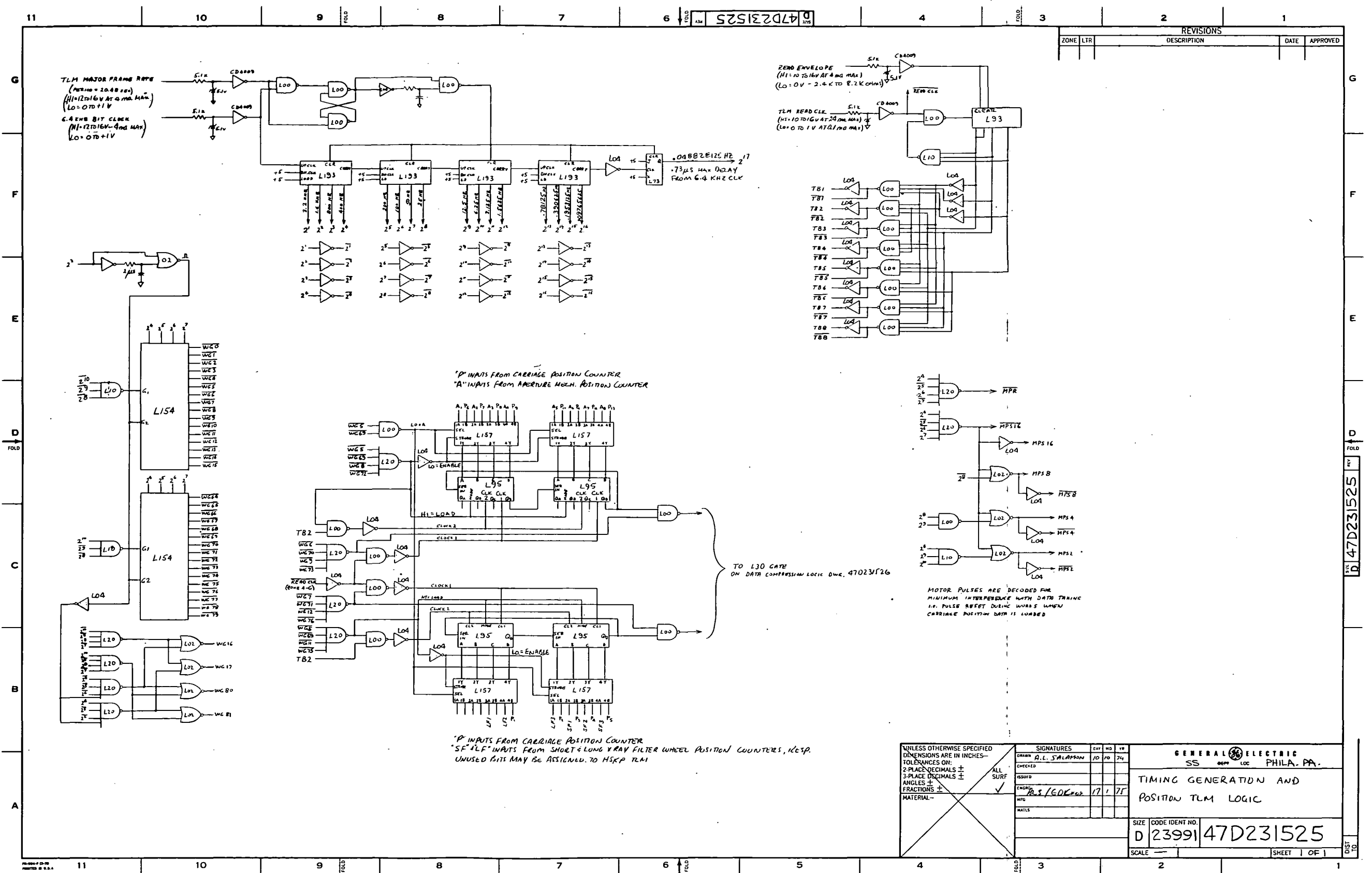
A description of the logic follows. Refer to "Timing Generation and Position TLM Logic" drawing 47D231525 which is included as Figure 3.7-1 and is referenced by zones in the following description.

In the upper left hand corner of Figure 3.7-1, the 6.4 KHz bit clock is counted down in a chain of 4 54L193 synchronous counters to generate all the required frequencies for decoding all events. This counting chain is synchronized to the TLM frame by using the "TLM Major Frame Rate" ($\approx .0488$ Hz) to reset the counters; the TLM frame starts when both inputs are in their HI to LO transition. In Zone B, C, D, E-10, all the pertinent word times are decoded by 54L154 decoders. Note that the word times decoded are based upon the word assignments assumed above; if the word assignments are changed, different word times have to be decoded. For each TLM word used, it is required that the word plus the word before (to start data compression), and the word after (to enable the data accumulation counter) be decoded.

In Zone F-4, the bit times are decoded by counting TLM read clock pulses and decoding the resultant count. The read envelope is used to reset the counter so that the trailing edge of the read envelope forces a count of 0 (TBI) rather than the 8th clock pulse---this is done by decoding a count of 7 and inhibiting further clock pulses. This is to satisfy the requirements of specification SS31331-400, page 111.

The pulses which start and stop motor pulses for the various stepping rates are decoded in Zones C, D-3, -4.

In the lower center of Figure 3.7-1 is the circuitry to sample carriage, filter wheel, and aperture wheel positions and put them on the data stream. Inputs marked P₁ through P₁₃ are the outputs of the carriage position up/down counter and are the binary equivalent of the position number at which the carriage is located at any given time. The carriage position is sampled during words 5 and 69 which is also the time when the Medium EUV data is read out;



REVISIONS				
ZONE	LTR	DESCRIPTION	DATE	APPROVED

UNLESS OTHERWISE SPECIFIED DIMENSIONS ARE IN INCHES—TOLERANCES ON: 2-PLACE DECIMALS ± 3-PLACE DECIMALS ± ANGLES ± FRACTIONS ± MATERIAL—	SIGNATURES	CHK	MD	TR
	DRAWN A.L. SALAPAN	10	10	74
	CHECKED			
	DESIGNED			
ENGINEER				
MFG				
MATERIAL				
GENERAL ELECTRIC SS PHILA. PA.				
TIMING GENERATION AND POSITION TLM LOGIC				
SIZE	CODE IDENT NO.			
D 23991	47D231525			
SCALE			SHEET	OF

Figure 3.7-1. Timing Generation and Position TLM Logic

thus the position corresponding to the data is known with maximum accuracy. The L00 gate (Zone D-9) decodes word gates 5 or 69 and selects the "B" inputs of the L157 "MUX ". The "MUX" is also strobed at that time by the L20 gate which "ORes" word gates 5, 69, 8 and 72. The outputs of this L20 gate are ANDed with TB2 producing a clock pulse to the L95 shift register loading the data on the trailing edge, i.e. at end of bit time 2. Note that the carriage position has 13 bits and that P₁ through P₅ are loaded as above, but through the lower multiplexer into the lower shift register---loading of both shift registers is simultaneous for carriage position data. The data is read out serially from the L95 shift registers by the "Read Clock" when it is enabled by the proper word gates (WG 6 and 70 for carriage position data P₁₃ through P₆; and WG 7 and 71 for P₅ through P₁, thus carriage position appears in adjacent words).

The filter wheel data (LF1 through LF3 and SF1 through SF3) and the aperture wheel position data (A₁ through A₈) is loaded and read out as described above except that it occurs at different times as a function of word gate inputs to the various gates.

The outputs of the shift registers go to the L30 OR gate shown on the data compression logic drawing where it is ORed with the science data and sent to the TLM system "Remote MUX".

3.8 ELECTRONICS PARTS

Table 3.8-1 lists the electronic parts which are different from those previously used on the OSO-7 instrument.

Table 3.8-1. New Electronics Parts

CD4001	SNC54L00
CD4002	SNC54L02
CD4008	SNC54L04
CD4009	SNC54L10
CD4010	SNC54L20
CD4011	SNC54L51
CD4012	SNC54L54
CD4015	SNC54L73
CD4017	SNC54L91
CD4019	SNC54L93
CD4021	SNC54L95
CD4023	SNC54L154
CD4025	SNC54L193
CD4027	
CD4029	
CD4042	
CD4047	SNC5407
CD4050	

3.9 COMMAND LIST

The command list for the new instrument is included as Appendix C. Changes from the OSO-7 command list are identified.

3.10 TELEMETRY LIST

The telemetry list for the new instrument is included as Appendix D. Changes from the OSO-7 telemetry list are identified.

3.11 LOGIC PACKAGING & POWER ESTIMATE

A study has been made which provides an estimate for the package size and power dissipation of the new logic generated during the study program. The low voltage power supply, five motor driver modules, and the motor regulator module are not included in the estimate, but are included in the total instrument power summary defined in Section 3.12.

It was assumed that the printed circuit boards would be approximately 6" x 4" and contain circuitry on both sides. The boards would be multi-layer, similar to S-193*types but slightly larger in area. The board connectors would be the S-193 type having 71 pins. Board spacing is 1/2 inch. Each board is assumed to contain a maximum of 48 16-pin flatpacks plus up to 20 discrete components (resistors, diodes, capacitors).

Based on the above assumptions, a circuit breakdown is made below and includes the power dissipation calculated from the final circuit design performed under the study contract.

Timing Generation and Housekeeping TLM Board. The board will contain 38 flatpacks, two of which are 24-pin types, plus 14 discrete components. The breakdown is as follows:

*SKYLAB S-193 EXPERIMENT

	<u>Number</u>	<u>Typical at 25°C</u>	<u>Power</u>	
				<u>Maximum Worst Case</u>
CD4009 (16 pin F.P.)	1	0.024 mw		0.1 mw
54L00 (14 pin F.P.)	6	24.0		45.5
54L04 (14 pin F.P.)	7	42.0		77.5
54L10 (14 pin F.P.)	1	3.0		4.9
54L20 (14 pin F.P.)	5	10.0		12.5
54L02 (14 pin F.P.)	2	11.0		22.1
54L73 (14 pin F.P.)	1	7.6		15.5
54L93 (14 pin F.P.)	1	16.0		35.6
54L95 (14 pin F.P.)	4	76.0		194.4
54L154 (24 pin F.P.)	2	170.0		270.0
54L157 (16 pin F.P.)	4	300.0		518.0
54L193 (16 pin F.P.)	<u>4</u>	<u>170.0</u>		<u>324.0</u>
TOTALS:	38	829.6 mw		1520.0 mw

- All power is from the Day Bus.
- The discrete components dissipate negligible power from the spectrohelio-graph power supply.

Data Accumulators, Compression Counter and Decoder Board #1

This board contains the data accumulators for 4 science data channels and the counter and decoder portion of the data compression circuit servicing these four data channels. It also contains the command relays for the X-Ray data modes (A, B or A-B).

			<u>Power</u>	
	<u>Number</u>	<u>Typical at 25°C</u>		<u>Maximum Worst Case</u>
54L00 (14 pin F.P.)	2	8 mw		15.1 mw
54L04 (14 pin F.P.)	3	18		33.3
54L10 (14 pin F.P.)	1	3		4.9
54L20 (14 pin F.P.)	2	4		7.6
54L51 (14 pin F.P.)	2	6		11.3
54L54 (14 pin F.P.)	14	35		68.0
54L93 (14 pin F.P.)	12	192		427.2
54L154 (24 pin F.P.)	1	85		135.0
54L193 (16 pin F.P.)	<u>5</u>	<u>212.5</u>		<u>405.0</u>
TOTALS:	42	563.5 mw		1107.4 mw

- In addition, there are 3 relays in T0-5 packages, 6 diodes, and 2 capacitors which dissipate negligible power from the spectroheliograph power supply.

- All power is from the Day Bus.

Data Accumulators, Compression Connector and Decoder Board #2

This board is identical to the above. It services the other 4 science data channels.

Data Compression Network and Mask Position Logic Board

This board contains both data compression circuits with the exception of the counters and decoders and the L30 gate which ORes all of the TLM signals and the 5407 TLM output buffer. It also contains the Mask Position Logic.

Data Compression Logic:

<u>Type</u>	<u>Number</u>	<u>Typical at 25°C</u>	<u>Power</u>	
				<u>Maximum Worst Case</u>
54L00 (14 pin F.P.)	8	32 mw		61.1 mw
54L04 (14 pin F.P.)	4	24		46.0
54L10 (14 pin F.P.)	7	21		40.3
54L20 (14 pin F.P.)	1	2		3.8
54L30 (14 pin F.P.)	9	9		20.4
54L51 (14 pin F.P.)	1	3		5.7
54L73 (14 pin F.P.)	3	22.8		46.6
54L91 (14 pin F.P.)	2	35		71.1
54L02 (14 pin F.P.)	1	5.5		11.3
5407 (14 pin F.P.)	1	108.5		167.0
Pull-up Resistor of 5407	1	12.5		15.0
Resistors	8	Negligible		Negligible
Capacitors	<u>10</u>	<u>Negligible</u>		<u>Negligible</u>
TOTALS:	37 F.P. + 19 Discrete	275.3 mw		488.3 mw

- All power is from the Day Bus

Mask Position Logic:

<u>Type</u>	<u>Number</u>	<u>Typical at 25°C</u>	<u>Power</u>	
				<u>Maximum Worst Case</u>
54L00 (14 pin F.P.)	1	4 mw		7.7 mw
54L04 (14 pin F.P.)	3	12 (half on night bus)		23.0 (half on night bus)
54L10 (14 pin F.P.)	1	3 (night bus)		5.8 (night bus)
54L20 (14 pin F.P.)	2	4		7.6
54L51 (14 pin F.P.)	1	3		5.7
54L54 (14 pin F.P.)	1	2.5		4.8
54L73 (14 pin F.P.)	<u>2</u>	<u>15.2</u>		<u>31.0</u>
TOTALS:	11	43.7 mw		85.6 mw

- Total power dissipation for the board is:

48 F.P. + 19 Discrete 310 mw typical Day Bus 556.6 mw worst case Day Bus

9 mw typical Night Bus 17.3 mw worst case Night Bus

(3 relays, 6 diodes, 2 resistors, and 2 capacitors associated with the Mask position logic must be located on another board)

X-Ray Filter Wheel Logic Board

This board contains the logic for both X-Ray filter wheels.

			<u>Power</u>	
<u>Type</u>	<u>Number</u>	<u>Typical at 25°C</u>	<u>Worst case</u>	<u>Maximum</u>
54L00 (14 pin F.P.)	6	24 mw		45.5 mw
54L04 (14 pin F.P.)	6	36		66.5
54L10 (14 pin F.P.)	1	3		4.9
54L20 (14 pin F.P.)	5	10		12.5
54L30 (14 pin F.P.)	4	4		9.0
54L51 (14 pin F.P.)	1	3		5.7
54L54 (14 pin F.P.)	2	5		9.6
54L73 (14 pin F.P.)	3	22.8		46.6
CD4010 (16 pin F.P.)*	3	Negligible		0.3
CD4012 (14 pin F.P.)*	2	Negligible		.03
CD4017 (16 pin F.P.)*	2	Negligible		3.0
CD4025 (14 pin F.P.)*	2	Negligible		.03
CD4042 (16 pin F.P.)*	4	Negligible		1.20
Resistors (13)		<u>50 mw</u>		<u>60.0</u>
TOTALS:	41	157.8 mw Day Bus < 1 mw Night Bus		260.2 mw Day Bus 4.56 mw Night Bus

The board also contains 6 T0-5 can relays, 5 capacitors, 13 resistors, and 12 diodes. (The remaining 10 relays, 28 diodes, and 10 resistors associated with

this circuitry must be located on another board.)

Aperture Wheel Logic Board

This board contains all the logic for the Aperture Wheel Drive plus the relays and discrete components left over from the Filter Wheel and Mask Position Logic (16 relays, 48 diodes, 17 resistors, 5 capacitors).

<u>Type</u>	<u>Number</u>	<u>Typical at 25°C</u>	<u>Power</u>	
			<u>Maximum Worst Case</u>	
54L00 (14 pin F.P.)	2	8 mw	15.3 mw	
54L04 (14 pin F.P.)	1	6	11.5	
54L10 (14 pin F.P.)	1	3	4.9	
54L20 (14 pin F.P.)	2	4	7.6	
Discrete Components	—	<u>80</u>	<u>93</u>	
TOTAL DAY BUS:	6	101 mw	132.3 mw	

<u>Type</u>	<u>Number</u>	<u>Typical at 25°C</u>	<u>Power</u>	
			<u>Maximum Worst Case</u>	
<u>NIGHT BUS ONLY</u>				
CD4008 (16 pin F.P.)	2	3.0 μ w	3.0 mw	
CD4009 (16 pin F.P.)	4	.2	.4	
CD4010 (16 pin F.P.)	2	.1	.2	
CD4011 (14 pin F.P.)	1	.005	.015	
CD4012 (14 pin F.P.)	2	.01	.03	
CD4015 (16 pin F.P.)	2	5.0	3.0	
CD4023 (14 pin F.P.)	2	.01	.03	
CD4029 (16 pin F.P.)	<u>3</u>	<u>4.5</u>	<u>4.5</u>	
TOTAL NIGHT BUS:	18	12.825 μ w	11.175 mw	

The relays and discrete components dissipate 80 mw typical and 93 mw worst case for the Day Bus.

Carriage Position Logic Boards (2)

The carriage position logic occupies two boards with some space left over for miscellaneous circuitry. The summary below does not attempt to partition the circuitry between the two boards, but treats the total power and part count for the carriage position logic.

DAY BUS:

<u>Type</u>	<u>Number</u>	<u>Power</u>	
		<u>Typical at 25°C</u>	<u>Maximum Worst Case</u>
54L00 (14 pin F.P.)	3	12 mw	23 mw
54L02 (14 pin F.P.)	1	5.5	8.6
54L04 (14 pin F.P.)	2	12	23
54L10 (14 pin F.P.)	2	6	9.8
54L20 (14 pin F.P.)	2	4	7.6
Resistors	17	1.5	1.7
Capacitors/Diodes	10/49	---	---
Relays	<u>6</u>	<u>---</u>	<u>---</u>
TOTALS:	10 F.P. + 82 discrete	41 mw	73.7 mw

NIGHT BUS:

CD4027 (16 pin F.P.)	1	.025 μ w	.3 mw
CD4047 (14 pin F.P.)	1	.25	.50
CD4001 (14 pin F.P.)	1	.005	.015
CD4002 (14 pin F.P.)	1	.005	.015
CD4008 (16 pin F.P.)	10	15.0	15.000
CD4009 (16 pin F.P.)	6	.3	.6
CD4010 (16 pin F.P.)	3	.15	.3
CD4011 (14 pin F.P.)	5	.025	.075
CD4012 (14 pin F.P.)	3	.015	.045

Night Bus (Continued)

<u>Type</u>	<u>Number</u>	<u>Power</u>	
		<u>Typical at 25°C</u>	<u>Maximum Worst Case</u>
CD4015 (16 pin F.P.)	4	10.0 μ W	6.0 mw
CD4019 (16 pin F.P.)	6	.9	9.0
CD4021 (16 pin F.P.)	2	5.0	3.0
CD4023 (14 pin F.P.)	4	.02	.06
CD4029 (16 pin F.P.)	<u>5</u>	<u>7.5</u>	<u>7.5</u>
TOTALS:	52	39.2 μ W	42.4 mw

The 50 KHz oscillator can be located on one of the carriage position boards.

The part count and power are:

Parts: 7 resistors, 2 diodes, 2 capacitors, 3 transistors

Power: 11.4 mw (Day Bus)

The Start of Line and Start of Raster input buffers can also be located on this board. Since we recommend using CMOS for these, buffers will use negligible power.

In summary, eight circuit boards will be required to package the logic circuitry defined by the study program. In addition, one additional board will be required to contain the circuitry for the H-Alpha filter heater controls. Packaging volume must also be provided for the low voltage power supply, five motor drive modules, and the motor regulator module.

3.12 INSTRUMENT POWER SUMMARY

The estimated power consumption for various operating modes has been calculated and are tabulated in Table 3.12-1. The summary is based on nominal part power dissipation at 25°C.

Table 3.12-1 Power Summary

	CONDITIONS*					
	1	2	3	4	5	6
+10 Volt	.12w	.12w	.12w	.12w	.12w	----
+5 Volt	2.61	2.78	2.65	2.62	2.62	.01w
Converter Loss (80% Eff)	.68	.73	.69	.69	.69	----
HVPS (6)(19V)	2.42	2.42	2.42	2.42	2.42	----
Heater/Controller (19V)	.23	.23	.23	.23	.23	.23
Motor Regulator (19V)	.18	.18	.18	.18	.18	----
Ent. Ap. Motor (19V)	----	1.98	----	----	----	----
Carriage Motor (19V)	----	1.98	.25	.25	.50	----
Mask Motor (19V)	----	1.98	----	----	----	----
SXR Motor (19V)	----	.99	.19	----	----	----
LXR Motor (19V)	----	.99	.19	----	----	----
TOTALS (WATTS):	6.24	14.38	6.92	6.51	6.76	.24

* Conditions

1. All experiments on, no motors stepping.
2. All experiments on, carriage and aperture mechanisms moving at 50 steps/sec, mask changing position, both filter wheels rotating at 25 steps/sec. (This condition may exist momentarily at orbit dawn due to commands sent during orbit night.)
3. All experiments on, aperture mechanism and mask stopped, carriage scanning at 6.25 steps/sec, filter wheels rotating one position each 5.12 sec (19% duty cycle).
4. All experiments on, aperture mechanism, mask, and filter wheels stopped,

carriage scanning at 6.25 steps/sec.

5. Same as condition 4 except carriage scanning at 12.5 steps/sec.
6. Orbit night.

The summaries in Table 3.12-1 are based on the following individual power calculations:

1. +10V power is 123 mw at all times
2. +5V power is 2.59 w (5V supply and no motors stepping)(see Section 3.11 for detail breakdown).
3. The 14V motor regulator dissipates .184 w of standby power with or without motors stepping.
4. +5V power for each motor driver is as follows:

@ 50 s/s	48 mw
@ 25 s/s	20.7 mw
@ 12.5 s/s	12.6 mw
@ 6.25 s/s	8.4 mw
stopped	4.3 mw
5. 19V power for each motor is as follows:

@ 50 s/s	1.98 w
@ 25 s/s	.99 w
@ 12.5 s/s	.495 w
@ 6.25 s/s	.25 w
stopped	0 w
6. Converter efficiency of 80% applies to +5V and +10V lines only
7. 19V power for H-Alpha Etalon heater and heater controls is as follows:

.200 w	- continuous power for control circuits
<u>.025 w</u>	- .100 watt heater at 25% duty cycle
.225 w	total

8. 19 volt power for High Voltage Power supplies is as follows:

1.500 w - 3 EUV at .500 w each

.250 w - LX-Ray

.290 w - SX-Ray

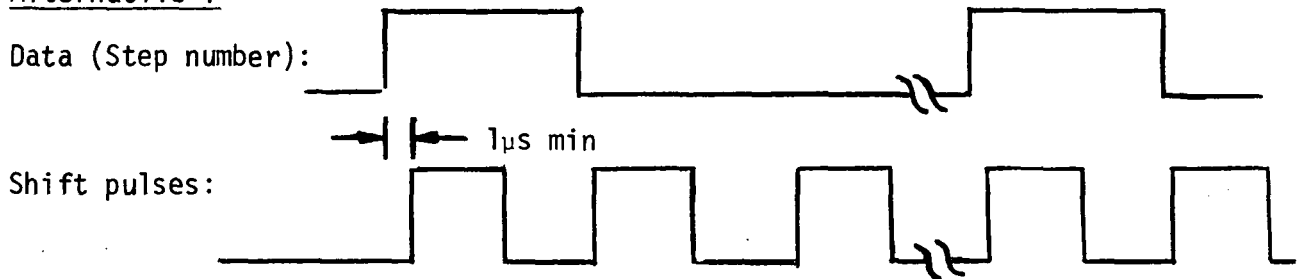
.380 w - H-Alpha

2.420 w - Total

3.13 POSITION COMMAND INTERFACE REQUIREMENTS

In commanding the carriage or the aperture mechanism to a given position, a number corresponding to the desired position must be sent from the spacecraft to the experiment. Two lines are required for each number (2 for the carriage position, and 2 for the aperture mechanism position), one line being the data (desired step number), and the other either a burst of shift clock pulses or a gate pulse (if the system clock is used). Two alternative interfaces are shown below; either one is equally acceptable to the experiment:

Alternative 1

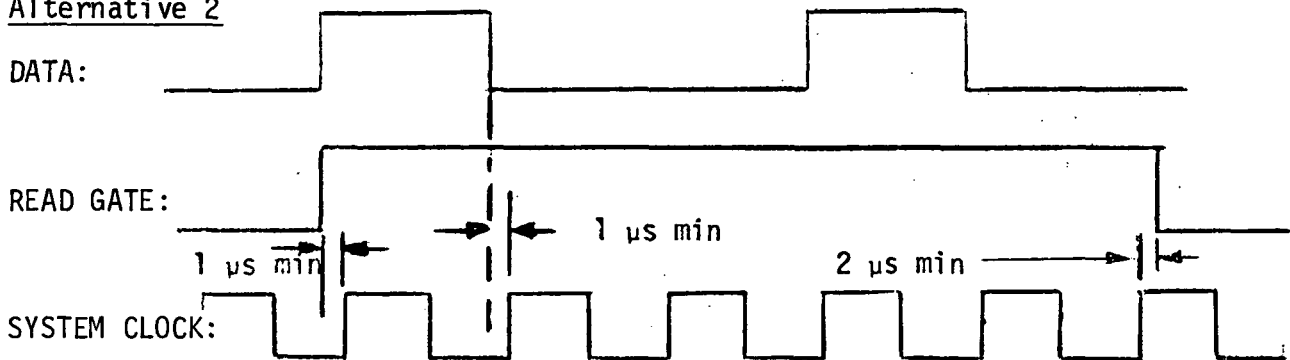


- Shift pulses must be low when not sending data and during orbit night (Day Bus off).
- Data shifted on rising edge of shift pulses
- Data must be in proper state and not changing from 1 μ s before rising edge of shift pulse until 1 μ s after rising edge of shift pulse.
- The number of shift pulses must be at least equal to the number of bits required (13 for the carriage and 8 for the aperture mechanism) or it may be greater provided the exact number of bits is specified and the location

of the data is specified (i.e. first 13 bits out of n bits). It is suggested, however, that no more than 16 pulses be used in order to minimize circuit count.

- e) Data may either be MSB first or LSB first as long as it is specified which by the time the board layouts are started.
- f) Minimum shift pulse width (HI state) is $1 \mu\text{s}$
- g) Maximum shift pulse rise and fall time is $5 \mu\text{s}$
- h) Voltage levels: HI = +3.5 to +5.5 V; LO = 0 to +0.4 V
- i) Current levels: HI = $100 \mu\text{a}$ maximum to experiment; LO = 1.8 ma maximum from experiment.

Alternative 2



In this scheme, the system clock is used to gate in the data in response to a "READ GATE" which enables this clock.

- a) "Read Gate" must go high at $1 \mu\text{s}$ (minimum) before a clock leading edge and go to LO $2 \mu\text{s}$ or more after a clock leading edge.
- b) Data must be in proper state and not changing $1 \mu\text{s}$ or more before and at least $2 \mu\text{s}$ after clock leading edge.
- c) Data is shifted in on rising edge of clock
- d, e, h, i) Same as for Alternative 1.

Since the shift pulses, clock, or read gate can be inverted in the experiment, the complements of these signals could be used (giving more flexibility to the

interface) provided that it is understood that inversion of the clock or shift pulses will change the timing requirements such that all references to rising edges will become falling edges.

Alternative 1 is used for the study program design.

3.14 SPECIAL SPACECRAFT-SPECTROHELIOGRAPH INTERFACE REQUIREMENT

An inherent problem exists in the spectroheliograph logic at power turn off; namely that the logic which keeps track of motor pulses (and thus motor position) responds in nanoseconds whereas the motor requires on the order of a 10 ms wide pulse to guarantee a step. Thus if the day bus is turned off after a motor pulse begins, the counter will respond and count that motor pulse, but the motor may or may not step depending on the width of the pulse, i.e., time from start of pulse to time when day bus decays. Various ways were examined to solve this problem within the instrument, but no satisfactory solution was found.

The preferred solution is to obtain a signal from the spacecraft which anticipates the day bus power shutdown. A logic signal from the spacecraft would be required to indicate when night is sensed and the day bus is about to be turned off. This logic signal must indicate "night" at least 20 ms before the day bus relay is opened. The logic signal should not present a problem since it must be available in the spacecraft; however, the 20 ms delay between this signal and actual day bus relay actuation may present a minor spacecraft design problem.

3.15 NON-VOLATILE MEMORY

The purpose of this study was to determine the availability of a suitable non-volatile memory system which could be incorporated into the new instrument

to prevent the loss of memory during power interruptions, especially during orbit night.

An extensive search was conducted to identify an appropriate off-the-shelf non-volatile memory system for use in the new instrument. Contacts with major suppliers of memory systems revealed that there are no suitable units currently available and that the development and qualification costs of such a unit would be prohibitive for an instrument type program. The manufacturers who were contacted are listed in Table 3.15-1.

As the result of this search, it was recommended that continuous power be obtained from the spacecraft for all critical logic/memory circuits and that these circuits be designed for minimum power consumption by using CMOS devices. This recommendation was approved by NASA/GSFC and was incorporated into the design of the logic for the new instrument. The continuous power required for the critical logic/memory circuits is approximately 10 milliwatts.

Table 3.15-1 Memory Systems Suppliers

<u>Core/Plated-wire Type</u>	<u>Semi-Conductor Type</u>
1. Honeywell/ASPD	1. Harris
2. Electronic Memories	2. Intel
3. Standard Memories	3. National
4. Ferroxcube	4. General Instruments
5. Ampex	5. NCR
6. Dataram	6. Hewlett-Packard
7. Space Crafts Incorporated	7. Advanced Memory Devices
8. Fabri-Tek	8. Monolithic Memories
	9. Texas Instruments

SECTION 4

EUV DETECTOR DEGRADATION STUDY

The OSO-7 EUV detection systems exhibited performance degradation after various periods in orbit. The purpose of this study is to analyze on-orbit data provided by NASA/GSFC and to determine possible causes for the observed degradation. Recommendations are made relative to the prevention of such faults in future applications.

4.1 STUDY SUMMARY

Figure 4.1-1 shows the comparative life histories of the three flight EUV detectors (Magnetic Electron Multipliers). Output intensity (count rate), in arbitrary units, is plotted against total accumulated counts. By the inspection of this plot, it is observed that the medium and long wavelength detectors exhibited a gradual loss in output count rate which is most likely caused by a gradual loss in gain. The short wavelength detector exhibited a rather abrupt loss in output count rate which would suggest either a mechanical or electrical failure within the detector or an electronic failure within the sensor electronics.

Figure 4.1-2 shows a typical loss in detector gain as a function of accumulated counts and threshold settings. The data used to construct Figure 4.1-2 was taken from laboratory tests conducted at NASA/GSFC using an Fe⁵⁵ radioisotope source.

Because Figure 4.1-1 suggests that life time may be a function of energy (or wavelength), the data of Figures 4.1-1 and 4.1-2 were plotted together in Figure 4.1-3 showing life vs. energy. Again, the short wavelength detector does not fit the pattern. The data from the other three detectors does suggest that the life expectancy may be less at higher energies.

Each of the three flight detectors was tested before launch according to the

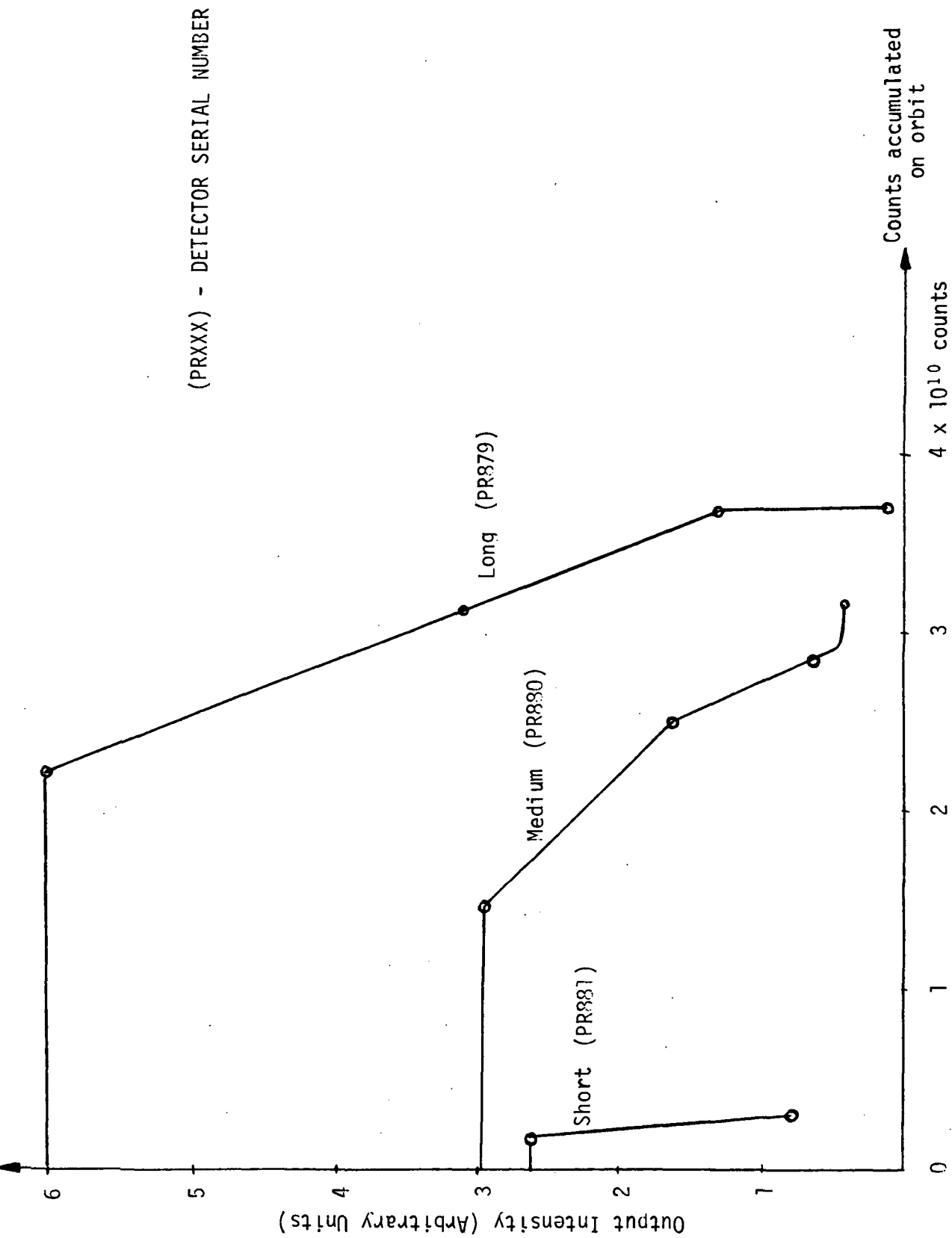


Figure 4.1-1. Life History for 3 MEMs on OSO-7

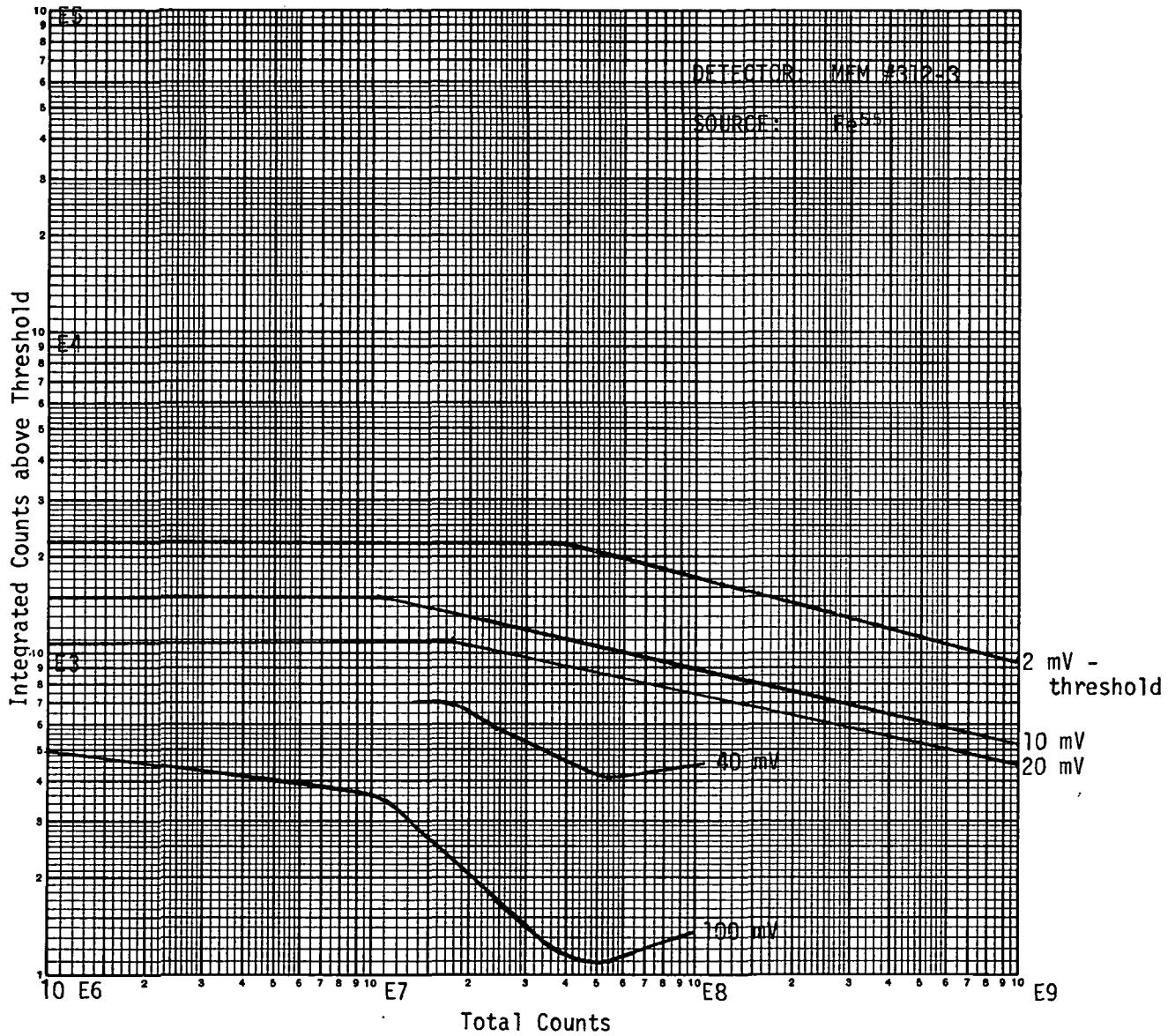


Figure 4.1-2. Life vs. Threshold Setting

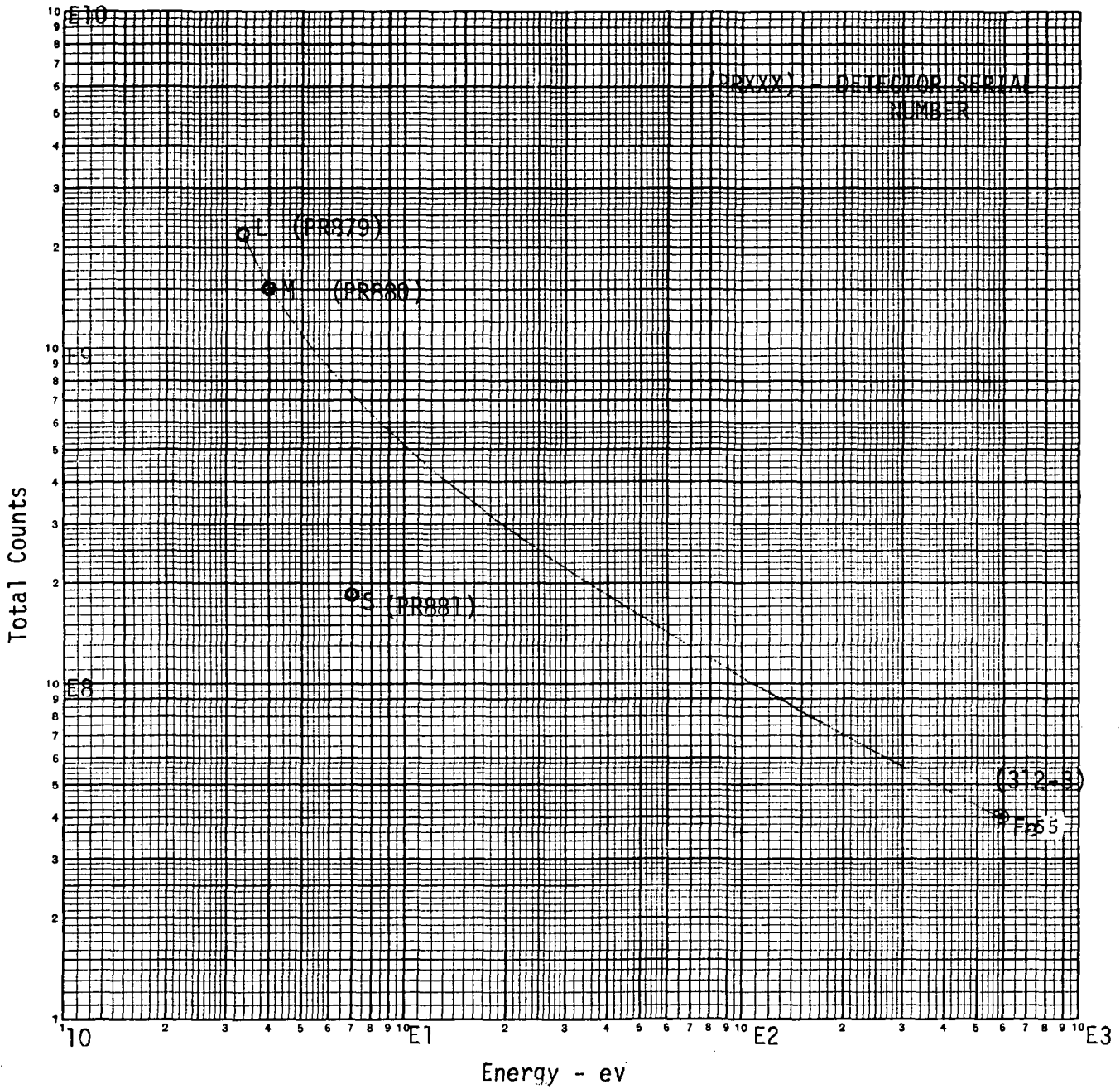


Figure 4.1-3. Life vs. Energy

standard test procedure. With this procedure, the detector is stimulated with an Fe⁵⁵ radioisotope source resulting in count rates of approximately 3000 cps. Count rate is then measured as a function of applied voltage resulting in so-called "plateau" curves.

The slope of the plateau curve is arbitrarily defined as the percentage change of count rate for a 100 V change in supply voltage. Also measured were threshold curves where the change in count rate is measured by varying the detection threshold from 0.1 to 1 V level with the high voltage set at the optimum point of the plateau curves. Table 4.1-1 shows the results.

Table 4.1-1
EUV Detector Plateau/Threshold Slopes

Counter	Plateau Slope %/100V	Threshold Slope Average .1 - 1V %/ .9V	Threshold Slope Average .1 - .3V %/ .2V
PR879 Long	2.45	12.5	.6
PR880 Medium	2.1	12.5	2.1
PR881 Short	5.13	28	11

Because only three detectors were measured, no definite correlation could be established between these measurements and life expectancy. However, because of the inference in the data, detectors with slopes deviating significantly from those of detectors PR879 and PR880 should be excluded for space applications.

4.2 CONCLUSIONS & RECOMMENDATIONS

The following conclusions were derived from the study:

1. The average life expectancy of a MEM is about 2×10^{10} counts.
2. Life expectancy (for equal incident flux) may change by a factor of 5 over the wavelength range from 12 to 64 nm, with a longer life expectancy at the

long wavelength end.

3. The short wavelength detector failed prematurely at 10% of its life expectancy.

Therefore, it is recommended that:

1. Limits on the acceptable plateau and threshold slopes for the EUV detectors should be tightened.
2. Compensation should be provided to account for the loss of detector output as a function of age by increasing the detector gain with an adjustable high voltage power supply which can be controlled from the ground or which is automatically controlled by the detector output.

SECTION 5

CALIBRATION AND TEST PROCEDURES

5.1 REQUIREMENTS

The purpose of this portion of the study program was to review the OSO-7 calibration and test procedures to identify changes to the procedures caused by the design changes generated by the study program.

5.2 PROCEDURE REVIEW SUMMARY

OSO-7 calibration and test procedures were reviewed for compatibility with the new spectroheliograph configuration defined by the study program. The results of the review are summarized in Table 5.2-1.

Table 5.2-1 Test Procedure Summary

Subsystem/Component	OSO-7 Test Procedure	Remarks
Magnetic Electron Multiplier	TI002	No change
Proportional Counter (SW)	TI003	No change
Proportional Counter (LW)	TI009	No change
PMT (H-Alpha)	TI004	May require revision based on final H-Alpha design.
Filter (H-Alpha)	None	New procedure required
EUV Telescope (GFE)	TI008	Revised procedure to be provided on Contract NAS5-23037
X-Ray Collimator (GFE)	TI006	May require revision based on final design
High Voltage Power Supplies	SVS7561	No change unless HVPS are GFE
Low Voltage Power Supply	1J86-OSOH-455	New procedure required for new LVPS design
Long X-Ray Filter Wheel	TI012	No change
Short X-Ray Filter Wheel	TI013	No change
EUV Carriage Assembly	TI011	No change
EUV Subsystem Calibration	TI016	Revision required to incorporate new step numbers and longer test wavelengths.
Instrument Test Procedure	1J86-OSOH-655	Extensive revision required due to changes to logic, LVPS, TLM, commands, and electrical interface.

SECTION 6
NEW TECHNOLOGIES

Monthly reviews of the work performed under the contract were conducted to identify items which fall within the reporting guidelines contained in the New Technology clause in the contract. No reportable items were identified.

PAGE INTENTIONALLY BLANK

APPENDICES

APPENDIX A

CONTRACT/REPORT CROSS REFERENCE SUMMARY

<u>Contract Specification Paragraph No.</u>	<u>GE Proposal Paragraph No.</u>	<u>Final Report Paragraph No.</u>
III-1	2.0	2.4, 2.6
-2	2.1.8	2.4
-3*	2.1.9*	---
-4	2.1.10	2.6
-5	2.5	5.0
-6	2.1.11	2.4, 2.5
-7	2.2.9	3.9, 3.10
-8	2.1.11, 2.2.10	2.5, 2.6.3, 3.8
IV -1*	2.2.1*	---
-2	2.1.1	2.1, 2.2, 2.3
-3	2.1.2	2.1, 2.2
-4	2.1.6	2.1
-5	2.2.2	3.6
-6	2.2.6	3.3
-7	2.1.3	2.1, 2.3
-8	2.1.4	2.3
-9	2.1.7	2.3
-10	2.2.5	2.1, 3.2
-11	2.2.5	2.1, 3.2
-12	2.2.6, 2.2	3.3, 2.4.2
-13	2.1.5	2.1
-14	2.2.6	3.3
-15	2.2.4	3.15
-16	2.2.7	3.4
-17*	2.2.7*	---
-18	2.2.8	3.5
-19	2.2.3	3.6
-20	2.3	4.0
-21*	2.4*	---
Mod 5 (Power Budget)	--	3.12
Mod 5 (Logic Diagram)	--	3.2, 3.3, 3.4, 3.5, 3.6,3.7

*Deleted

APPENDIX B

EUV ENTRANCE SLIT ANALYSIS

The following writeup is essentially a transcript of an analysis done by Dr. W. M. Neupert, NASA/GSFC.

The geometry of the concave diffraction grating is shown schematically in Figure B-1.

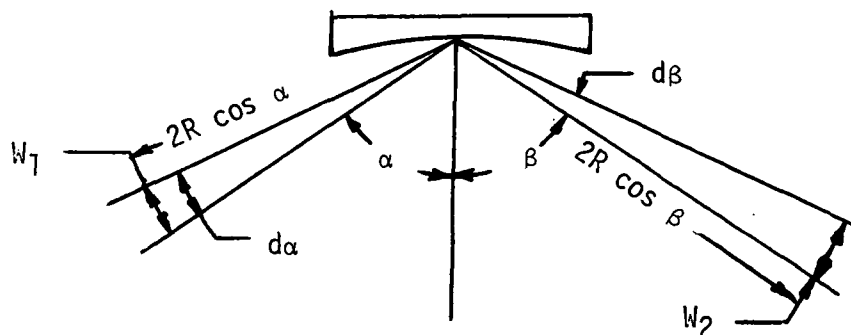


Figure B-1

Diffraction Grating Schematic

Where R is the radius of the Rowland circle.

The wavelength is given by

$$\eta \lambda = a (\sin \alpha - \sin \beta)$$

where: η = diffraction order

a = grating constant

It follows:

$$\eta d \lambda = a (\cos \alpha d \alpha - \cos \beta d \beta)$$

and
$$d \alpha = \frac{W_1}{2R \cos \alpha} \quad \text{and} \quad d \beta = \frac{W_2}{2R \cos \beta}$$

$$\cos \alpha = \frac{W_1}{2R d \alpha} \quad \cos \beta = \frac{W_2}{2R d \beta}$$

Substituting;
$$\eta d \lambda = a \left(\frac{W_1}{2R} - \frac{W_2}{2R} \right)$$

For $\eta = 1$ the full line width is given by

$$\Delta\lambda_T = \frac{aW}{R} \times 10^7 \text{ nm}$$

and substituting: $a = \frac{1}{11520} \text{ cm}$

$$W = 2 \times 10^{-3} \times 2.54 \text{ cm}$$

$$R = 50 \text{ cm}$$

$$\Delta\lambda_T = .088 \text{ nm } (.88 \text{ \AA})$$

The scan step size is .0072 nm (.072 Å) on the average. This corresponds to 12.2 steps per full width or 6.1 steps per half width, which means that a shift of one step or .0072 nm will be detectable. The allowable shift in entrance slit corresponding to one step follows as

$$l = \frac{\Delta\lambda(2R)}{a} \quad \text{or}$$

$$l = .0072 \times 10^{-7} \times 100 \times 11520 = 8.29 \times 10^{-4} \text{ cm} = 8.29 \text{ } \mu\text{m}$$

Allowing for a safety factor, the allowable tolerance is +3 μm. This tolerance could, however, be relaxed for the larger slit; therefore, it may be desirable from a tolerance control standpoint to place all of the high resolution slits at one end of the vertical slit.

APPENDIX C
SPECTROHELIOGRAPH STUDY
PRELIMINARY COMMAND LIST

	<u>OSO-7</u>	<u>NEW</u>
<u>I. EUV & H-ALPHA SYSTEMS</u>		
1. READOUT H-ALPHA & SHORT EUV	✓	-
2. READOUT MEDIUM & LONG EUV	✓	-
3. SWITCH BETWEEN (1) & (2) ABOVE FOR EOR	✓	-
4. FAST SPECTRAL SCAN (12.5 STEPS/SEC)	✓	✓
5. SLOW SPECTRAL SCAN (6.25 STEPS/SEC)	✓	✓
6. ADVANCE CARRIAGE TO LONG EUV END & STOP (50 STEPS/SEC) (ALSO STOPS SCAN ITEMS 4, 5, & 9)	✓	✓
7. ADVANCE CARRIAGE TO SHORT EUV END & STOP (50 STEPS/SEC) (ALSO STOPS SCAN ITEMS 4, 5, & 9 & RESETS LOGIC)	✓	✓
8. ADVANCE CARRIAGE TO A SELECTED STEP NUMBER & STOP (50 STEPS/SEC) ALSO STOPS SCAN ITEMS 4, 5, & 9	-	✓
9. SCAN +128 STEPS ABOUT SELECTED STEP NUMBER START SCAN TOWARD LONG EUV END SCAN AT 6.25 STEPS/SEC	-	✓
10. ADVANCE CARRIAGE 1 STEP TOWARD LONG EUV END & STOP	✓	-
11. ADVANCE CARRIAGE 1 STEP TOWARD SHORT EUV END & STOP	✓	-
12. CHANGE MASK POSITION	✓	-
13. SELECT MASK POSITION A	-	✓
14. SELECT MASK POSITION B	-	✓
15. SWITCH MASK AT END OF EACH RASTER	✓	✓
16. STOP SPECTRAL SCAN	-	✓
17. STEP APERTURE WHEEL 1 STEP	✓	-
18. SCAN APERTURE WHEEL (6.25 STEPS/SEC)	✓	✓
19. STOP SCAN OF APERTURE WHEEL	✓	✓
20. RETURN TO REFERENCE (NARROWEST SLIT/#1)	✓	✓

I. EUV & H-ALPHA SYSTEMS (Continued) OSO-7 NEW

21. ADVANCE APERTURE WHEEL TO SELECTED STEP NUMBER AT 50 STEPS/SEC AND STOP - ✓

II. LONG WAVELENGTH X-RAY SYSTEM OSO-7 NEW

- | | | | |
|-----|---|---|---|
| 1. | READOUT LXR CHANNEL A ONLY | ✓ | ✓ |
| 2. | READOUT LXR CHANNEL B ONLY | ✓ | ✓ |
| 3. | READOUT LXR CHANNEL A-B ONLY | ✓ | ✓ |
| 4. | ADVANCE LXR FILTER WHEEL 1 POSITION | ✓ | - |
| 5. | ADVANCE LXR & SXR FILTER WHEELS
1 POSITION EACH 5.12 SEC | ✓ | ✓ |
| 6. | ADVANCE LXR FILTER WHEEL 1 POSITION
AT EOR | ✓ | ✓ |
| 7. | ADVANCE LXR F/W TO POSITION 1 FROM ANY POSITION**
(position 1 is reference position) | - | ✓ |
| 8. | ADVANCE LXR F/W TO POSITION 2 FROM ANY POSITION** | - | ✓ |
| 9. | " " " " " 3 " " " ** | - | ✓ |
| 10. | " " " " " 4 " " " ** | - | ✓ |
| 11. | " " " " " 5 " " " ** | - | ✓ |
| 12. | " " " " " 6 " " " ** | - | ✓ |

** 25 steps/sec; also stops auto advance in item 5 & 6 above

III. SHORT WAVELENGTH X-RAY SYSTEM

(SAME AS DESCRIBED FOR LONG WAVELENGTH X-RAY SYSTEM IN SECTION II EXCEPT COMMAND 5 DOES NOT NEED TO BE REPEATED)

IV. LOW VOLTAGE POWER SUPPLY

- | | | | |
|----|------------------------------------|---|---|
| 1. | SWITCH TO LAUNCH POWER | ✓ | - |
| 2. | SWITCH TO DAY POWER | ✓ | - |
| 3. | LV ON/OFF---PROVIDED BY SPACECRAFT | ✓ | ✓ |

OSO-7

NEW

V. HIGH VOLTAGE POWER SUPPLIES

1. S EUV & L EUV HV ON	✓	-
2. M EUV HV ON	✓	✓
3. H-ALPHA HV ON	✓	✓
4. L X-RAY HV ON	✓	✓
5. S X-RAY HV ON	✓	✓
6. POLARIMETER HV ON	✓	-
7. EUV & H-ALPHA OFF	✓	✓
8. L X-RAY, S X-RAY & POLARIMETER OFF	✓	-
9. S EUV HV ON	-	✓
10. L EUV HV ON	-	✓
11. L X-RAY & S X-RAY HV OFF	-	✓

NOTE: Additional commands to select voltage levels TBD

APPENDIX D
SPECTROHELIOGRAPH STUDY
PRELIMINARY TELEMETRY LIST

<u>MAIN FRAME DATA</u>	<u>OSO-7</u>	<u>NEW</u>
1. EUV SHORT WAVELENGTH CHANNEL	✓ (1)	✓
2. EUV MEDIUM WAVELENGTH CHANNEL	✓ (1)	✓
3. EUV LONG WAVELENGTH CHANNEL	✓ (1)	✓
4. H-ALPHA CHANNEL	✓ (1)	✓
5. LONG WAVELENGTH X-RAY CHANNEL A	--	✓
6. LONG " " " A, or B, or A-B	✓	✓
7. SHORT " " " A	--	✓
8. SHORT " " " A, or B, or A-B	✓	✓
9. APERTURE WHEEL STEP NUMBER	--	✓
10. CARRIAGE STEP NUMBER (~4650 STEPS)	--	✓
11. MASK POSITION	--	✓
12. L X-RAY FILTER WHEEL POSITION	--	✓
13. S X-RAY FILTER WHEEL POSITION	--	✓
14. END OF LINE SCAN	✓	✓ (2)
15. END OF RASTER SCAN	✓	✓ (2)
16. END OF SPECTRAL SCAN	✓	✓ (2)
 <u>SUB FRAME DATA</u>		
1. POLARIMETER CHANNEL A	✓	--
2. " " B	✓	--
3. " " C	✓	--

SUB FRAME DATA (Continued)

	<u>OSO-7</u>	<u>NEW</u>
4. LVPS VOLTAGE	✓	✓
5. HVPS #1 VOLTAGE	--	✓
6. HVPS #2 VOLTAGE	--	✓
7. HVPS #3 VOLTAGE	--	✓
8. HVPS #4 VOLTAGE	--	✓
9. HVPS #5 VOLTAGE	--	✓
10. HVPS #6 VOLTAGE	--	✓
11. TEMPERATURE #1 (TELESCOPE)	✓	✓
12. TEMPERATURE #2 (COLL-FWD)	--	✓
13. TEMPERATURE #3 (COLL-AFT)	--	✓
14. TEMPERATURE #4 (APERTURE WHEEL)	✓	✓
15. TEMPERATURE #5 (GRATING)	--	✓
16. TEMPERATURE #6 (TRACK)	--	✓
17. TEMPERATURE #7 (TRACK)	--	✓
18. TEMPERATURE #8 (ELECTRONICS BOX)	✓	✓
19. SHORT X-RAY CHANNEL A ONLY INDICATOR	✓	✓
20. SHORT " " B ONLY INDICATOR	✓	✓
21. SHORT " " A-B ONLY INDICATOR	✓	✓
22. LONG " " A ONLY INDICATOR	✓	✓
23. LONG " " B ONLY INDICATOR	✓	✓
24. LONG " " A-B ONLY INDICATOR	✓	✓
25. SHORT X-RAY FILTER WHEEL POSITION	✓	-- (3)
26. LONG X-RAY FILTER WHEEL POSITION	✓	-- (3)
27. EUV MASK POSITION	✓	-- (3)

SUB FRAME DATA (Continued)

	<u>OSO-7</u>	<u>NEW</u>
28. DIRECTION OF SPECTRAL SCAN	✓	--
29. SPECTRAL SCAN-STOPPED OR MOVING	✓	--
30. APERTURE WHEEL POSITION	✓	-- (3)
31. H-ALPHA & SHORT EUV OR LONG & MED EUV SELECTION	✓	--
32. SELECTED CARRIAGE STEP POSITION (INCLUDES CENTRAL STEP POSITION FOR MINI-SCAN)	-	✓

(1) SHORT EUV & H-ALPHA OR MEDIUM & LONG EUV

(2) CHANGE TO USE SEPARATE MAIN FRAME WORD--DELETE CODING INTO DATA CHANNELS

(3) INCLUDED UNDER MAIN FRAME DATA